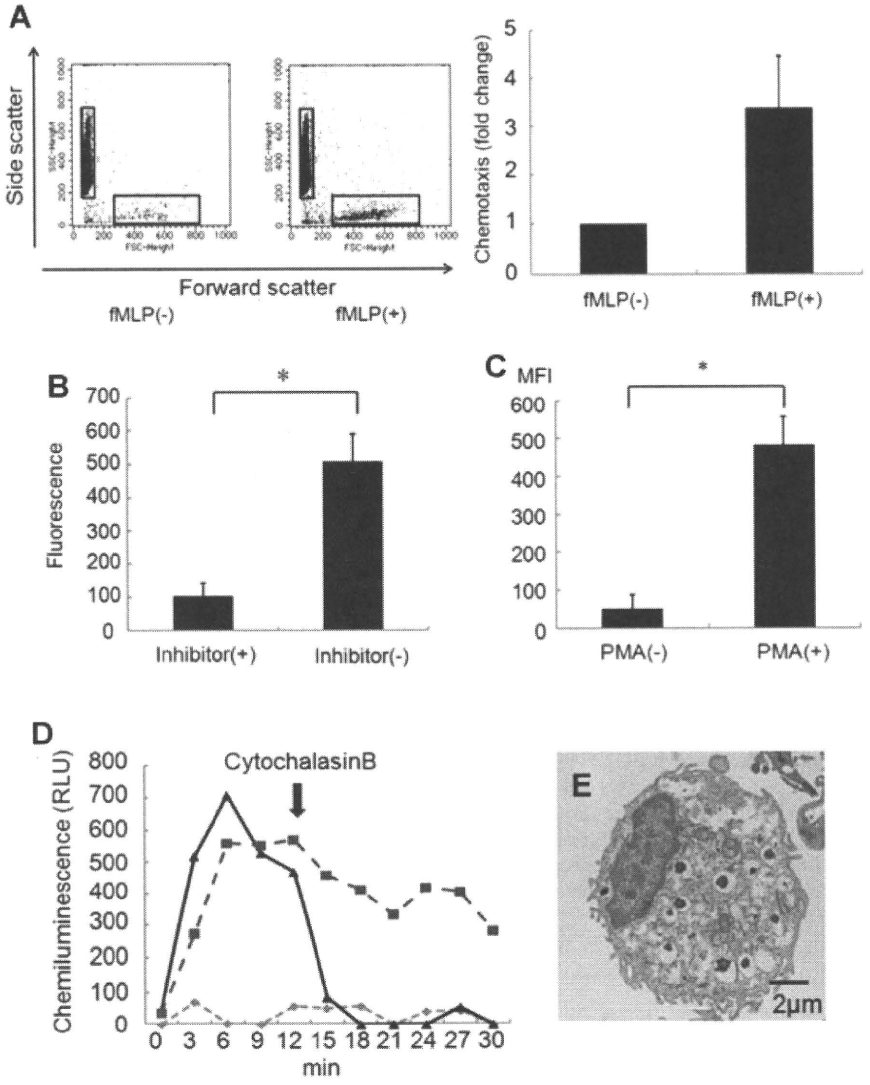

Fig. 3. Functional analysis of hiPSC-derived neutrophils. (A) Chemotactic activity of floating cells on day10 + 30 in response to fMLP was determined as described in Materials and Methods section. After a 4-h culture, the transwell inserts were removed, and the cells in the lower chamber were counted by an LSR flow cytometer (n = 3; bars represent SDs). (B) MPO chlorination activity in cell lysates from floating cells on day10 + 30 was analyzed by EnzChek Myeloperoxidase (MPO) Activity Assay Kit as described in the Materials and Methods section. The chlorination activity in neutrophil cell lysates was almost completely abolished by the addition of a chlorination inhibitor (n = 3; bars represent SDs; *$P < 0.05$.). (C) Floating cells on day10 + 30 were subjected to DHR assay. DHR was reacted with neutrophils with or without PMA, and the resultant rhodamine fluorescence was detected by flow cytometry. The addition of PMA increased the levels of fluorescence. Results are expressed as mean fluorescence intensity (MFI) (n = 3; bars represent SDs; *$P < 0.05$.). (D) Floating cells on day10 + 30 were subjected to the assay for phagocytosis-induced respiratory burst activity using chemiluminescent microspheres (luminol-binding microspheres). Gradual increase in chemiluminescence indicates the respiratory burst triggered by the phagocytosis of luminol-binding microspheres (squares). The increase in chemiluminescence was almost completely abolished by the addition of cytochalasin B (diamonds) and inhibited by its later addition (triangles). The figures are representative of three independent experiments. Abbreviation: RLU, relative light units. (E) hiPSC-derived neutrophils phagocytosing the microbeads were analyzed by transmission electron microscopy.

differentiation in this culture system were investigated by RT-PCR (Fig. 4E–F). NANOG, a pluripotency marker, was expressed in undifferentiated iPS cells but disappeared in sorted VEGFR2^{high}CD34^{+} cells after 10 days differentiation. PU.1 and C/EBPα, essential transcription factors for commitment and differentiation of the granulocytic lineage (Borregaard et al., 2001; Friedman, 2007) were first detected on day 10 + 10 and persisted thereafter. C/EBPε, which had a critical role for the later stages of neutrophil development and transcription of key granule proteins (Borregaard et al., 2001; Friedman, 2007) were first detected faintly on day 10 + 10 and upregulated thereafter. MPO and lactoferrin, which were expressed at the highest levels in myeloblasts/promyelocytes and myelocytes/metamyelocytes, respectively (Cowland and Borregaard, 1999; Borregaard et al., 2001), were detected on day 10 + 10. Gelatinase, which was expressed at the highest level in band and segmented neutrophilic cells (Cowland and Borregaard, 1999; Borregaard et al., 2001), was first detected on day 10 + 20 and upregulated thereafter. Altogether, these results suggested that the neutrophil differentiation in this co-culture system might recapitulate the orderly differentiation process in bone marrow.

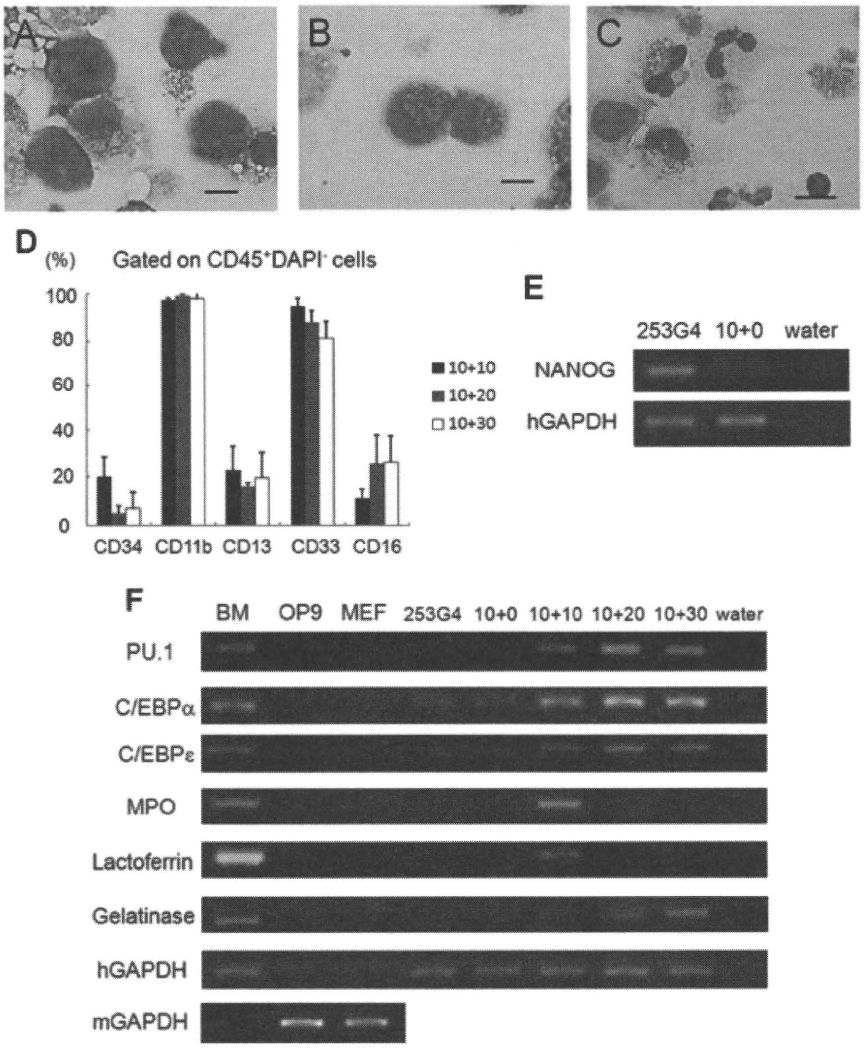

Fig. 4. Sequential analysis of neutrophil differentiation from hiPSCs. (A–C) Sequential morphological analysis of day10 + 10 (A), day10 + 20 (B) and day10 + 30 (C). Scale bars: 10 μm. (D) Surface antigen expression at each level of differentiation of hiPSC-derived cells was analyzed by flow cytometry. All adherent cells including OP9 cells were harvested and stained with antibodies. Human $CD45^{+}DAPI^{-}$ cells were gated as hiPSC-derived viable leukocytes (n = 3; bars represent SDs). (E–F) Sequential RT-PCR analysis of a pluripotency marker (E), genes associated with neutrophil development and neutrophils-specific granules (F) during differentiation. Human GAPDH was used as a loading control. Abbreviations: BM, human bone marrow cells; 253G4, undifferentiated 253G4 cells; 10 + 0, sorted $VEGFR2^{high}CD34^{+}$ cells after 10 days differentiation; 10 + 10, 20, 30, all cells after 10, 20, 30 days differentiation after cell sorting; hGAPDH, human GAPDH; mGAPDH, mouse GAPDH. The figures are representative of three independent experiments. [Color figure can be viewed in the online issue, which is available at wileyonlinelibrary.com.]

Discussion

The analysis of the differentiation process of neutrophils can provide helpful information for the elucidation of the pathogenesis of hematopoietic diseases that affect neutrophils and/or myeloid differentiation, including inherited bone marrow failure syndromes and neutrophil function disorders. Traditionally, HL-60, an acute promyelocytic cell line, has been used as a neutrophil differentiation model (Collins et al., 1978; Newburger et al., 1979). Although this cell line grows well and differentiates easily into neutrophils, the neutrophil differentiation model is not suitable for the analysis of neutrophil-affected disorders because of its leukemic cell-origin. Development of a neutrophil differentiation system based on iPS cells would provide a better model for the analysis of such diseases, because iPS cells can be generated from the somatic cells of patients suffering from these diseases.

The current study aimed to investigate two issues in hiPSC-derived neutrophil differentiation: tracking the step-wise maturation in vitro and evaluating the wide spectrum of neutrophil functions. Through the use of a modified OP9 co-culture system, the directed and step-wise differentiation from hiPSCs to mature neutrophils containing neutrophil specific granules was first accomplished. The expression of surface antigens, transcription factors and granule proteins during differentiation exhibited the characteristic pattern of normal granulopoiesis. The biological functions of hiPSC-derived neutrophils were demonstrated through the quantitative assessment of granule enzyme activities and biological bactericidal activities such as chemotaxis and phagocytosis.

Defects in the maturation and function of neutrophils are associated with certain blood diseases including inherited bone marrow failure syndromes and neutrophil function disorders.

Among bone marrow failure syndromes, certain conditions affect a specific maturation stage, such as the maturation arrest at the plomyelocyte/myelocyte stage seen in severe congenital neutropenia. Neutrophil function disorders can affect specific bactericidal activities, such as the absence of MPO activity characteristic of MPO deficiency disorders. The use of hiPSCs for the investigation of these diseases requires sequential analyses that can identify each neutrophil maturation stage and include a functional analysis to evaluate each bactericidal activity separately on disease-specific, iPSC-derived neutrophils. Although previous studies have reported neutrophil differentiation models from hESCs (Choi et al., 2009; Saeki et al., 2009; Yokoyama et al., 2009) and hiPSC-derived neutrophils have been shown before (Choi et al., 2009), evidence showing that hiPSCs, which are artificially reprogrammed somatic cells, can follow the normal developmental pathway into fully functional mature neutrophils is of great significance, and the description of methods for identifying each neutrophil maturation step and analyzing each bactericidal pathway separately is important for clinical applications.

Although flow-cytometric analysis combined with RT-PCR identified the neutrophil maturation step relatively successfully, discrepancies between the neutrophil differentiation system in this study and normal granulopoiesis were noted such as the lower expression of CD16 than that shown by previous reports on hESC-derived neutrophils (Choi et al., 2009; Saeki et al., 2009; Yokoyama et al., 2009). As CD16 is a mature neutrophil marker in peripheral blood, two reasons could explain this phenomenon. First, residual precursors could have been more significant contaminants in the present system than in previously reported methods due to the function of cytokines and stroma supporting immature hematopoietic cells. Another possible reason is the shift of protein types between membrane-bound and soluble forms. Calluri previously reported that G-CSF is not only a myeloid cell growth factor, but also a modulator of neutrophil behavior (Carulli, 1997), and its stimulation decreases the membrane bound CD16 and increases its soluble form. Low CD16 expression has been documented in neutrophils derived in vitro from bone marrow $CD34^+$ cells by stimulation with G-CSF (Kerst et al., 1993b), and it has been observed in vivo when G-CSF is administered to healthy volunteers (Kerst et al., 1993a). This phenomenon, which is also documented in a report of hESC-derived neutrophils (Yokoyama et al., 2009), is unavoidable in differentiation culture systems using recombinant cytokines. The combination of flow cytometric and PCR analyses enables a more accurate staging of progenitors that could be of importance in the investigation of maturation arrest in future studies.

The culture system presented in this study is considered ineligible for clinical applications due to the use of xenogeneic factors such as OP9 cells and FCS. To overcome this problem, a xeno-free hematopoietic differentiation system from pluripotent cells is currently being established.

In conclusion, the present study shows the establishment of a fully functional mature neutrophil differentiation system from hiPSCs and the detailed analysis of their function and differentiation process. This system could become a useful tool for the investigation of various hematological diseases with defects in maturation and function of neutrophils.

Acknowledgments

We thank Dr. Yamanaka for providing the human iPS cell lines 201B6, 253G1, and 253G4, and Dr. Kodama for providing the OP9 cells. We are grateful to Kyowa Hakko Kirin for providing IL-3, TPO, and G-CSF. We also thank the Center for Anatomical Studies, Kyoto University Graduate School of Medicine for immunocytochemical analysis and transmission electron microscopy analysis. This work was supported by grants from the Ministry of Education, Culture, Sports, Science and Technology, Japan. This work was also supported by the Global COE Program "Center for Frontier Medicine" by the Ministry of Education, Culture, Sports, Science, and Technology (MEXT), Japan.

References

Agarwal S, Loh YH, McLoughlin EM, Huang J, Park IH, Miller JD, Huo H, Okuka M, Dos Reis RM, Loewer S, Ng HH, Keefe DL, Goldman FD, Klingelhutz AJ, Liu L, Daley GQ. 2010. Telomere elongation in induced pluripotent stem cells from dyskeratosis congenita patients. Nature 464:292–296.

Alter BP. 2007. Diagnosis, genetics, and management of inherited bone marrow failure syndromes. Hematology Am Soc Hematol Educ Program 29–39.

Borregaard N, Cowland JB. 1997. Granules of the human neutrophilic polymorphonuclear leukocyte. Blood 89:3503–3521.

Borregaard N, Theilgaard-Monch K, Sorensen OE, Cowland JB. 2001. Regulation of human neutrophil granule protein expression. Curr Opin Hematol 8:23–27.

Boyden S. 1962. The chemotactic effect of mixtures of antibody and antigen on polymorphonuclear leucocytes. J Exp Med 115:453–466.

Carulli G. 1997. Effects of recombinant human granulocyte colony-stimulating factor administration on neutrophil phenotype and functions. Haematologica 82:606–616.

Choi KD, Vodyanik MA, Slukvin II. 2009. Generation of mature human myelomonocytic cells through expansion and differentiation of pluripotent stem cell-derived lin-CD34+CD43+CD45+ progenitors. J Clin Invest 119:2818–2829.

Collins SJ, Ruscetti FW, Gallagher RE, Gallo RC. 1978. Terminal differentiation of human promyelocytic leukemia cells induced by dimethyl sulfoxide and other polar compounds. Proc Natl Acad Sci USA 75:2458–2462.

Cowland JB, Borregaard N. 1999. The individual regulation of granule protein mRNA levels during neutrophil maturation explains the heterogeneity of neutrophil granules. J Leukoc Biol 66:989–995.

Duan Z, Horwitz M. 2003. Targets of the transcriptional repressor oncoprotein Gfi-1. Proc Natl Acad Sci USA 100:5932–5937.

Evans MJ, Kaufman MH. 1981. Establishment in culture of pluripotential cells from mouse embryos. Nature 292:154–156.

Friedman AD. 2007. Transcriptional control of granulocyte and monocyte development. Oncogene 26:6816–6828.

Harvath L, Falk W, Leonard EJ. 1980. Rapid quantitation of neutrophil chemotaxis: use of a polyvinylpyrrolidone-free polycarbonate membrane in a multiwell assembly. J Immunol Methods 37:39–45.

Kerst JM, de Haas M, van der Schoot CE, Slaper-Cortenbach IC, Kleijer M, von dem Borne AE, van Oers RH. 1993a. Recombinant granulocyte colony-stimulating factor administration to healthy volunteers: induction of immunophenotypically and functionally altered neutrophils via an effect on myeloid progenitor cells. Blood 82:3265–3272.

Kerst JM, van de Winkel JG, Evans AH, de Haas M, Slaper-Cortenbach IC, de Wit TP, von dem Borne AE, van der Schoot CE, van Oers RH. 1993b. Granulocyte colony-stimulating factor induces hFc gamma RI (CD64 antigen)-positive neutrophils via an effect on myeloid precursor cells. Blood 81:1457–1464.

Kholodnyuk ID, Kozireva S, Kost-Alimova M, Kashuba V, Klein G, Imreh S. 2006. Down regulation of 3p genes, LTF, SLC38A3 and DRR1, upon growth of human chromosome 3-mouse fibrosarcoma hybrids in severe combined immunodeficiency mice. Int J Cancer 119:99–107.

Lensch MW, Daley GQ. 2006. Scientific and clinical opportunities for modeling blood disorders with embryonic stem cells. Blood 107:2605–2612.

Meissner A, Wernig M, Jaenisch R. 2007. Direct reprogramming of genetically unmodified fibroblasts into pluripotent stem cells. Nat Biotechnol 25:1177–1181.

Mori Y, Iwasaki H, Kohno K, Yoshimoto G, Kikushige Y, Okeda A, Uike N, Niiro H, Takenaka K, Nagafuji K, Miyamoto T, Harada M, Takatsu K, Akashi K. 2009. Identification of the human eosinophil lineage-committed progenitor: revision of phenotypic definition of the human common myeloid progenitor. J Exp Med 206:183–193.

Nakagawa M, Koyanagi M, Tanabe K, Takahashi K, Ichisaka T, Aoi T, Okita K, Mochiduki Y, Takizawa N, Yamanaka S. 2008. Generation of induced pluripotent stem cells without Myc from mouse and human fibroblasts. Nat Biotechnol 26:101–106.

Newburger PE, Chovaniec ME, Greenberger JS, Cohen HJ. 1979. Functional changes in human leukemic cell line HL-60. A model for myeloid differentiation. J Cell Biol 82:315–322.

Niwa A, Umeda K, Chang H, Saito M, Okita K, Takahashi K, Nakagawa M, Yamanaka S, Nakahata T, Heike T. 2009. Orderly hematopoietic development of induced pluripotent stem cells via Flk-1(+) hemoangiogenic progenitors. J Cell Physiol 221:367–377.

Okita K, Ichisaka T, Yamanaka S. 2007. Generation of germline-competent induced pluripotent stem cells. Nature 448:313–317.

Park IH, Arora N, Huo H, Maherali N, Ahfeldt T, Shimamura A, Lensch MW, Cowan C, Hochedlinger K, Daley GQ. 2008a. Disease-specific induced pluripotent stem cells. Cell 134:877–886.

Park IH, Zhao R, West JA, Yabuuchi A, Huo H, Ince TA, Lerou PH, Lensch MW, Daley GQ. 2008b. Reprogramming of human somatic cells to pluripotency with defined factors. Nature 451:141–146.

Raya A, Rodriguez-Piza I, Guenechea G, Vassena R, Navarro S, Barrero MJ, Consiglio A, Castella M, Rio P, Sleep E, Gonzalez F, Tiscornia G, Garreta E, Aasen T, Veiga A, Verma IM, Surralles J, Bueren J, Izpisua Belmonte JC., 2009. Disease-corrected haematopoietic progenitors from Fanconi anaemia induced pluripotent stem cells. Nature 460:53–59.

Saeki K, Nakahara M, Matsuyama S, Nakamura N, Yogiashi Y, Yoneda A, Koyanagi M, Kondo Y, Yuo A. 2009. A feeder-free and efficient production of functional neutrophils from human embryonic stem cells. Stem Cells 27:59–67.

Shinoda G, Umeda K, Heike T, Arai M, Niwa A, Ma F, Suemori H, Luo HY, Chui DH, Torii R, Shibuya M, Nakatsuji N, Nakahata T. 2007. alpha4-Integrin(+) endothelium derived from primate embryonic stem cells generates primitive and definitive hematopoietic cells. Blood 109:2406–2415.

Sugimoto C, Fujieda S, Sunaga H, Noda I, Tanaka N, Kimura Y, Saito H, Matsukawa S. 2001. Granulocyte colony-stimulating factor (G-CSF)-mediated signaling regulates type IV collagenase activity in head and neck cancer cells. Int J Cancer 93:42–46.

Suwabe N, Takahashi S, Nakano T, Yamamoto M. 1998. GATA-1 regulates growth and differentiation of definitive erythroid lineage cells during in vitro ES cell differentiation. Blood 92:4108–4118.

Takahashi K, Tanabe K, Ohnuki M, Narita M, Ichisaka T, Tomoda K, Yamanaka S. 2007. Induction of pluripotent stem cells from adult human fibroblasts by defined factors. Cell 131:861–872.

Takahashi K, Yamanaka S. 2006. Induction of pluripotent stem cells from mouse embryonic and adult fibroblast cultures by defined factors. Cell 126:663–676.

Toda Y, Kono K, Abiru H, Kokuryo K, Endo M, Yaegashi H, Fukumoto M. 1999. Application of tyramide signal amplification system to immunohistochemistry: a potent method to localize antigens that are not detectable by ordinary method. Pathol Int 49:479–483.

Tulpule A, Lensch MW, Miller JD, Austin K, D'Andrea A, Schlaeger TM, Shimamura A, Daley GQ. 2010. Knockdown of Fanconi anemia genes in human embryonic stem cells reveals early developmental defects in the hematopoietic lineage. Blood 115:3453–3462.

Uchida T, Kanno T, Hosaka S. 1985. Direct measurement of phagosomal reactive oxygen by luminol-binding microspheres. J Immunol Methods 77:55–61.

Umeda K, Heike T, Yoshimoto M, Shinoda G, Shiota M, Suemori H, Luo HY, Chui DH, Torii R, Shibuya M, Nakatsuji N, Nakahata T. 2006. Identification and characterization of hemoangiogenic progenitors during cynomolgus monkey embryonic stem cell differentiation. Stem Cells 24:1348–1358.

Umeda K, Heike T, Yoshimoto M, Shiota M, Suemori H, Luo HY, Chui DH, Torii R, Shibuya M, Nakatsuji N, Nakahata T. 2004. Development of primitive and definitive hematopoiesis from nonhuman primate embryonic stem cells in vitro. Development 131:1869–1879.

van de Winkel JG, Anderson CL. 1991. Biology of human immunoglobulin G Fc receptors. J Leukoc Biol 49:511–524.

van Lochem EG, van der Velden VH, Wind HK, te Marvelde JG, Westerdaal NA, van Dongen JJ. 2004. Immunophenotypic differentiation patterns of normal hematopoiesis in human bone marrow: reference patterns for age-related changes and disease-induced shifts. Cytometry B Clin Cytom 60:1–13.

Vowells SJ, Sekhsaria S, Malech HL, Shalit M, Fleisher TA. 1995. Flow cytometric analysis of the granulocyte respiratory burst: a comparison study of fluorescent probes. J Immunol Methods 178:89–97.

Winterbourn CC. 2002. Biological reactivity and biomarkers of the neutrophil oxidant, hypochlorous acid. Toxicology 181-182:223–227.

Yokoyama Y, Suzuki T, Sakata-Yanagimoto M, Kumano K, Higashi K, Takato T, Kurokawa M, Ogawa S, Chiba S. 2009. Derivation of functional mature neutrophils from human embryonic stem cells. Blood 113:6584–6592.

Yu J, Vodyanik MA, Smuga-Otto K, Antosiewicz-Bourget J, Frane JL, Tian S, Nie J, Jonsdottir GA, Ruotti V, Stewart R, Slukvin II, Thomson JA. 2007. Induced pluripotent stem cell lines derived from human somatic cells. Science 318:1917–1920 .

Published November 22, 2010

Transient activation of *c-MYC* expression is critical for efficient platelet generation from human induced pluripotent stem cells

Naoya Takayama,[1] Satoshi Nishimura,[3,4,5] Sou Nakamura,[1] Takafumi Shimizu,[2] Ryoko Ohnishi,[1] Hiroshi Endo,[1,2] Tomoyuki Yamaguchi,[2] Makoto Otsu,[2] Ken Nishimura,[4,6] Mahito Nakanishi,[6] Akira Sawaguchi,[7] Ryozo Nagai,[3,5] Kazutoshi Takahashi,[8] Shinya Yamanaka,[8] Hiromitsu Nakauchi,[2] and Koji Eto[1]

[1]Stem Cell Bank and [2]Division of Stem Cell Therapy, Center for Stem Cell Biology and Regenerative Medicine, the Institute of Medical Science, and [3]Department of Cardiovascular Medicine and [5]Translational Systems Biology and Medicine Initiative, the University of Tokyo, Tokyo 113-0033, Japan
[4]PRESTO, Japan Science and Technology Agency, Tokyo 102-8666, Japan
[6]Gene Function Research Center, National Institute of Advanced Industrial Science and Technology, Ibaraki 305-8562, Japan
[7]Department of Anatomy, University of Miyazaki Faculty of Medicine, Miyazaki 889-1692, Japan
[8]Center for iPS Research and Application, Kyoto University, Kyoto 606-8507, Japan

Human (h) induced pluripotent stem cells (iPSCs) are a potentially abundant source of blood cells, but how best to select iPSC clones suitable for this purpose from among the many clones that can be simultaneously established from an identical source is not clear. Using an in vitro culture system yielding a hematopoietic niche that concentrates hematopoietic progenitors, we show that the pattern of *c-MYC* reactivation after reprogramming influences platelet generation from hiPSCs. During differentiation, reduction of *c-MYC* expression after initial reactivation of c-MYC expression in selected hiPSC clones was associated with more efficient in vitro generation of $CD41a^+CD42b^+$ platelets. This effect was recapitulated in virus integration-free hiPSCs using a doxycycline-controlled c-MYC expression vector. In vivo imaging revealed that these $CD42b^+$ platelets were present in thrombi after laser-induced vessel wall injury. In contrast, sustained and excessive *c-MYC* expression in megakaryocytes was accompanied by increased p14 (*ARF*) and p16 (*INK4A*) expression, decreased *GATA1* expression, and impaired production of functional platelets. These findings suggest that the pattern of *c-MYC* expression, particularly its later decline, is key to producing functional platelets from selected iPSC clones.

CORRESPONDENCE
K. Eto:
keto@ims.u-tokyo.ac.jp

Abbreviations used: CB, cord blood; DOX, doxycycline; ESC, embryonic stem cell; HDF, human dermal fibroblast; HLA, human leukocyte antigen; iPSC, induced pluripotent stem cell; KO, Kusabira orange; MK, megakaryocyte; PB, peripheral blood; SCF, stem cell factor; Tg, transgene; TPO, thrombopoietin; VEGF-R2, vascular endothelial growth factor type 2 receptor.

Platelets are key elements not only of hemostasis and thrombosis but also of tissue regeneration after injury and the pathophysiology of inflammation (Gawaz et al., 2005; Nesbitt et al., 2009). The production of platelets, thrombopoiesis, is regulated primarily by thrombopoietin (TPO)-mediated megakaryopoiesis within the BM (Patel et al., 2005; Schulze and Shivdasani, 2005). Notably, many patients with critical thrombocytopenia, caused by dysregulation of BM as a result of hematopoietic disease or aggressive chemotherapy, require platelet transfusions using platelet concentrates obtained through blood donation (Webb and Anderson, 1999). It is well known, however, that repeated transfusion induces antibodies in recipients against allogenic human leukocyte antigen (HLA) on the transfused platelets (Schiffer, 2001). To establish a supply of identical platelet concentrates without loss of responsiveness as a result of immunorejection, particularly for patients with a rare HLA, human (h) induced pluripotent stem cells (iPSCs) represent a potentially abundant source.

Successful reprogramming of differentiated fibroblasts into a pluripotent stage using the defined genes *OCT3/4*, *KLF4*, *SOX2*, and *c-MYC* (Takahashi et al., 2007; Yu et al., 2007) is a potentially effective means of generating HLA-matched iPSCs for regenerative medicine

The Rockefeller University Press $30.00
J. Exp. Med. Vol. 207 No. 13 2817-2830
www.jem.org/cgi/doi/10.1084/jem.20100844

Supplemental Material can be found at:
http://jem.rupress.org/content/suppl/2010/11/22/jem.20100844.DC1.html

Published November 22, 2010

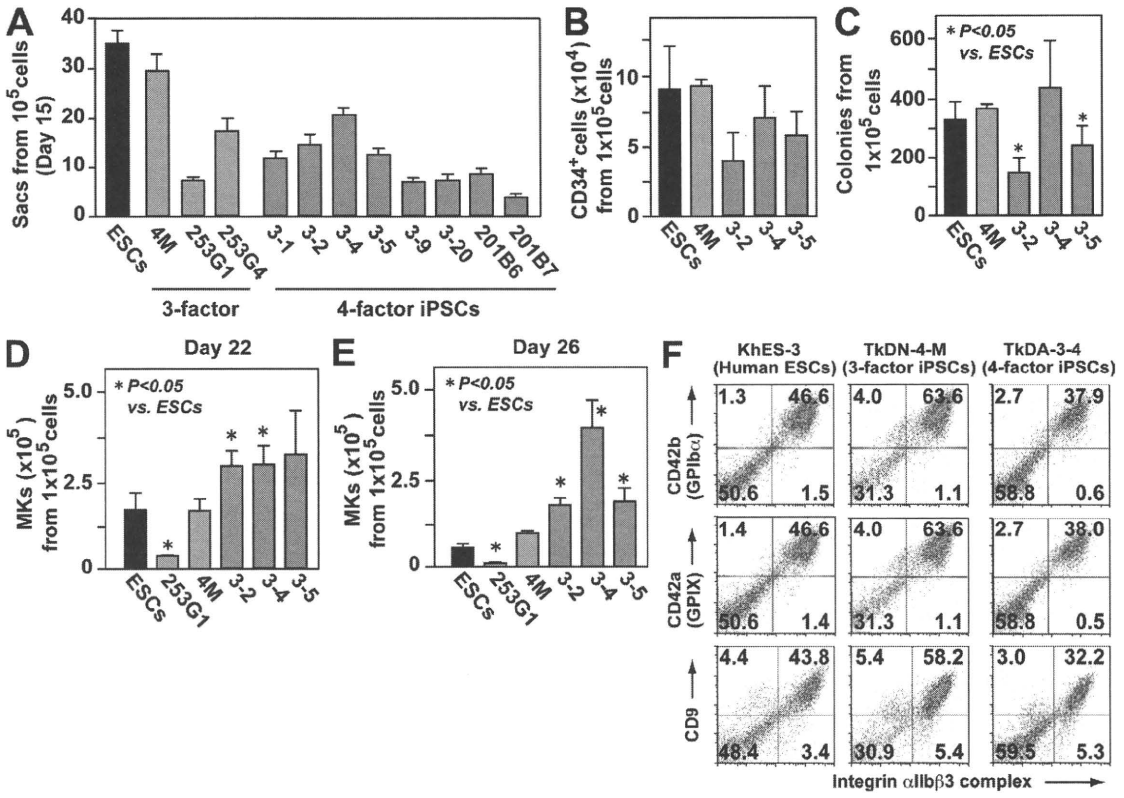

Figure 1. Four-factor human iPSCs are better than three-factor iPSCs for megakaryopoiesis, which is independent of hematopoietic colony potential. (A) Numbers of ESC- and iPSC-sac-like structures generated from 10^5 cells ($n = 3$, means ± SEM from three independent experiments). (B) Numbers of CD34$^+$ hematopoietic progenitors within ESC- or iPSC-sacs yielded from 10^5 human ESCs or iPSCs ($n = 3$, means ± SEM). (C) Numbers of hematopoietic colonies derived from 10^5 human ESCs or iPSCs within sacs ($n = 3$, means ± SEM). (D and E) Numbers of CD42b (GPIbα)$^+$ MKs derived from 10^5 hematopoietic progenitors within sacs on day 22 (D) and day 26 (E; $n = 5$, means ± SEM). (F) Representative flow cytometry dot plots for khES-3-, TkDN-4-M-, and TkDA3-4-derived MKs examined on day 24.

(Raya et al., 2009). However, reactivation of *c-Myc* during establishment of iPSCs can reportedly lead to oncogenicity after transplantation (Okita et al., 2007). But because platelets are anucleate, they can be irradiated before transfusion to eliminate residual hiPSCs or other differentiated nucleated cells that could form teratomas or malignant tumors (van der Meer and Pietersz, 2005). Thus, platelet concentrates derived from hiPSCs could be a useful source of HLA-identical platelets, which eliminates the need for scarce donor blood. That said, because a large number of iPSC clones can be simultaneously generated from an identical source, the iPSC clone most suitable for the desired purpose must be selected before the differentiation phase (Miura et al., 2009). We therefore sought to determine the hallmark of such cells as well as the best way to select iPSC clones in vitro for generation of functional platelets in vivo.

c-Myc plays essential roles in both embryonic and adult hematopoiesis, although its effects on megakaryopoiesis and thrombopoiesis in various mouse models remains unclear (Thompson et al., 1996a,b; Chanprasert et al., 2006; Guo et al., 2009). For example, two studies of inducible *c-Myc* overexpression (O/E) under the control of megakaryocyte (MK)-specific differentiation revealed that *c-Myc* plays a positive role in the proliferation of MK progenitors (Thompson et al., 1996a,b). Moreover, *c-Myc* is reportedly essential for the TPO–c-mpl axis in megakaryopoiesis (Chanprasert et al., 2006). In contrast, recent studies using *c-Myc*–deficient mice showed that the absence of the gene actually led to an increase in the platelet count (Guo et al., 2009).

Using a culture system that yields an in vitro hematopoietic niche containing hematopoietic progenitors (which we named iPS-Sac), we show in this paper that limited reactivation of *c-MYC* and its subsequent decline after a reactivation-dependent increase in the gene's expression in immature MKs are key components of platelet generation in vitro and contribute to the selection and validation of iPSC clones in which genome integration is accomplished through reprogramming. These clones are suitable for transfusion in clinical applications or mechanistic studies of thrombopoiesis using disease-specific iPSCs.

RESULTS

Four-factor hiPSC-derived hematopoietic progenitors contribute to enhanced generation of MKs and platelets

Using VSV-G–pseudotyped retroviruses (Ory et al., 1996) harboring human reprogramming factors (*OCT3/4*, *SOX2*,

Published November 22, 2010

KLF4, and/or *c-MYC*), we sought to establish iPSCs from human dermal fibroblasts (HDFs). With our system, we consistently generated 200–300 hiPSC clones from 10^5 HDFs. For evaluation of pluripotency, established iPSC clones obtained through transduction with four or three factors (with or without *c-MYC*) and all clones showing a normal karyotype (not depicted) were examined for morphology, SSEA-4 expression (Fig. S1 A), other gene expression (Fig. S1 B), and the ability to form teratomas in vivo (Fig. S1 C). Our findings confirmed that exogenous *OCT3/4*, *SOX2*, *KLF4*, and *c-MYC* remained unexpressed in established iPSCs (Fig. S1 B).

To explore the hiPSC clones' potential for differentiation into hematopoietic cells (Takayama et al., 2008), we evaluated several iPS-Sacs (Fig. S2 A) from individual clones (four-factor hiPSCs: TkDA3-1, -2, -4, -5, -9, -20, 201B6, and 201B7; three-factor hiPSCs: TkDN4-M, 253G1, and 253G4) and compared them to previously evaluated human (h) embryonic stem cells (ESCs; KhES3 clone, Kyoto University, Japan; Takayama et al., 2008). On day 15 of culture, iPS-Sacs that contained numerous hematopoietic-like round cells (Fig. S2 B) and showed expression of vascular endothelial growth factor type 2 receptor (VEGF-R2$^+$; Fig. S2 B) or platelet endothelial cell adhesion molecule 1 (CD31$^+$; not depicted) were deemed to be potentially suitable microenvironments from which to obtain hematopoietic progenitors, as was observed in hESC-derived structures (Takayama et al., 2008).

We detected considerable heterogeneity in the production of iPS-Sacs (a hallmark of the efficiency of hematopoietic progenitors) from iPSCs derived from the same source (i.e., TkDA3-1, -2, -4, -5, -9, or -20; Fig. 1 A), which was also consistent with previous observations in hESCs (Osafune et al., 2008). In particular, CD34$^+$, but not CD34$^-$, cells from iPS-Sacs showed successful colony formation in methylcellulose colony assays (Fig. S2 C). The three-factor clone TkDN4-M, as well as KhES-3, appeared to have a greater potential for myeloid lineage hematopoiesis, as exemplified by the numbers of Sacs (Fig. 1 A, red bar) composed of CD34$^+$ cells (Fig. 1 B, red bar), and the numbers of hematopoietic colonies formed from each Sac (Fig. 1 C, red bar). Nonetheless, the number of CD42b (GPIbα; von Willebrand factor receptor)$^+$ MKs obtained with four-factor iPSC clones (e.g., TkDA3-2, TkDA3-4, and TkDA3-5) was higher than that obtained with TkDN4-M or KhES-3 when equal numbers of cells from iPS-Sacs were seeded onto fresh culture dishes in the presence of TPO, stem cell factor (SCF), and heparin (Fig. 1, D [day 22] and E; and Fig. S3 day 26; Takayama et al., 2008). For example, clone TkDA3-4 generated three times as many MKs as TkDN4-M or KhES-3 at the peak of production (Fig. 1 E, day 26; and Fig. S3). By days 22–38, phase-contrast imaging revealed the presence of proplatelets, a prerelease platelet form (Video 1), as well as mature MKs by May-Giemsa staining (Fig. S4). Moreover, flow cytometric analysis showed that 40–60% of floating cells expressed CD41a (integrin αIIbβ3 complex), a fibrinogen receptor, as well as CD42a (GPIX), GPIbα, and CD9, all of which are hallmarks of MKs (Fig. 1 F; Tomer, 2004; Takayama et al., 2008).

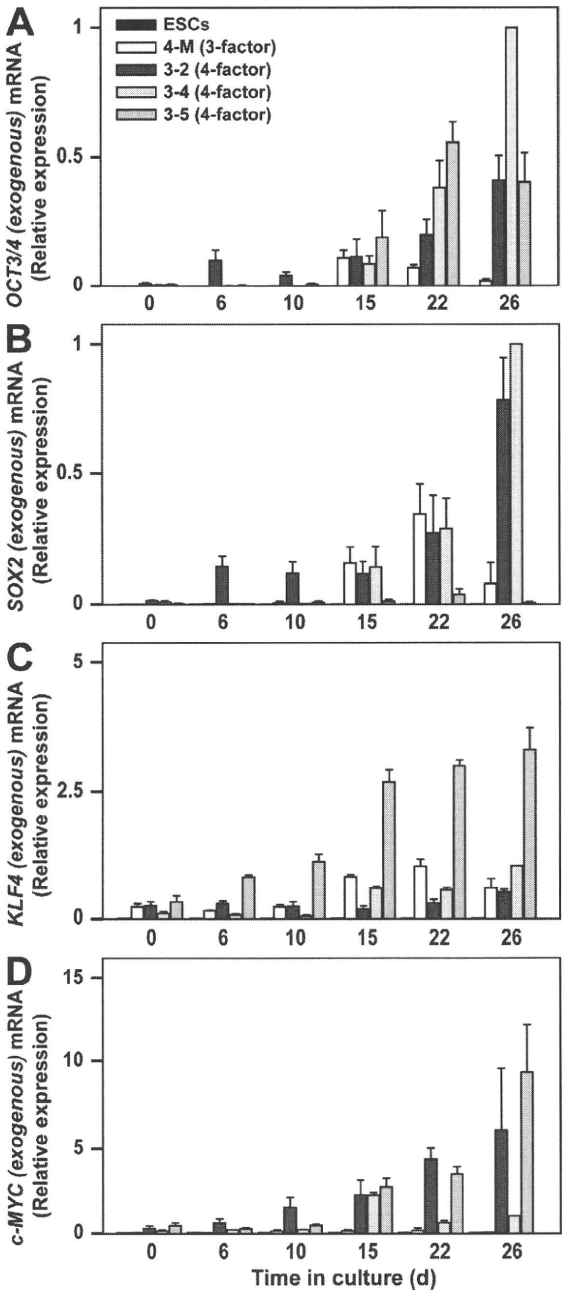

Figure 2. Time-dependent changes in qPCR induced by exogenous reprogramming genes in three-factor or four-factor iPSCs. mRNA encoding exogenous *OCT3/4* (A), *SOX2* (B), *KLF4* (C), *and c-MYC* (D) in human ES cells (ESCs), TkDN4-M (three-factor iPSCs), TkDA3-2, TkDA3-4, and TkDA3-5 (four-factor iPSCs) on day 0 or their derivatives (on days 6, 10, 15, 22, and 26 after initiation of MK-lineage culture) were examined by qPCR as described in the Materials and methods section. TkDA3-4–derived mature MKs (day 26) was assigned a value of 1.0 ($n = 4$, means ± SEM from two independent experiments).

To determine the mechanism underlying the enhanced megakaryopoiesis exhibited by four-factor hiPSC-derived hematopoietic progenitors, we assessed the potential of progenitors

Published November 22, 2010

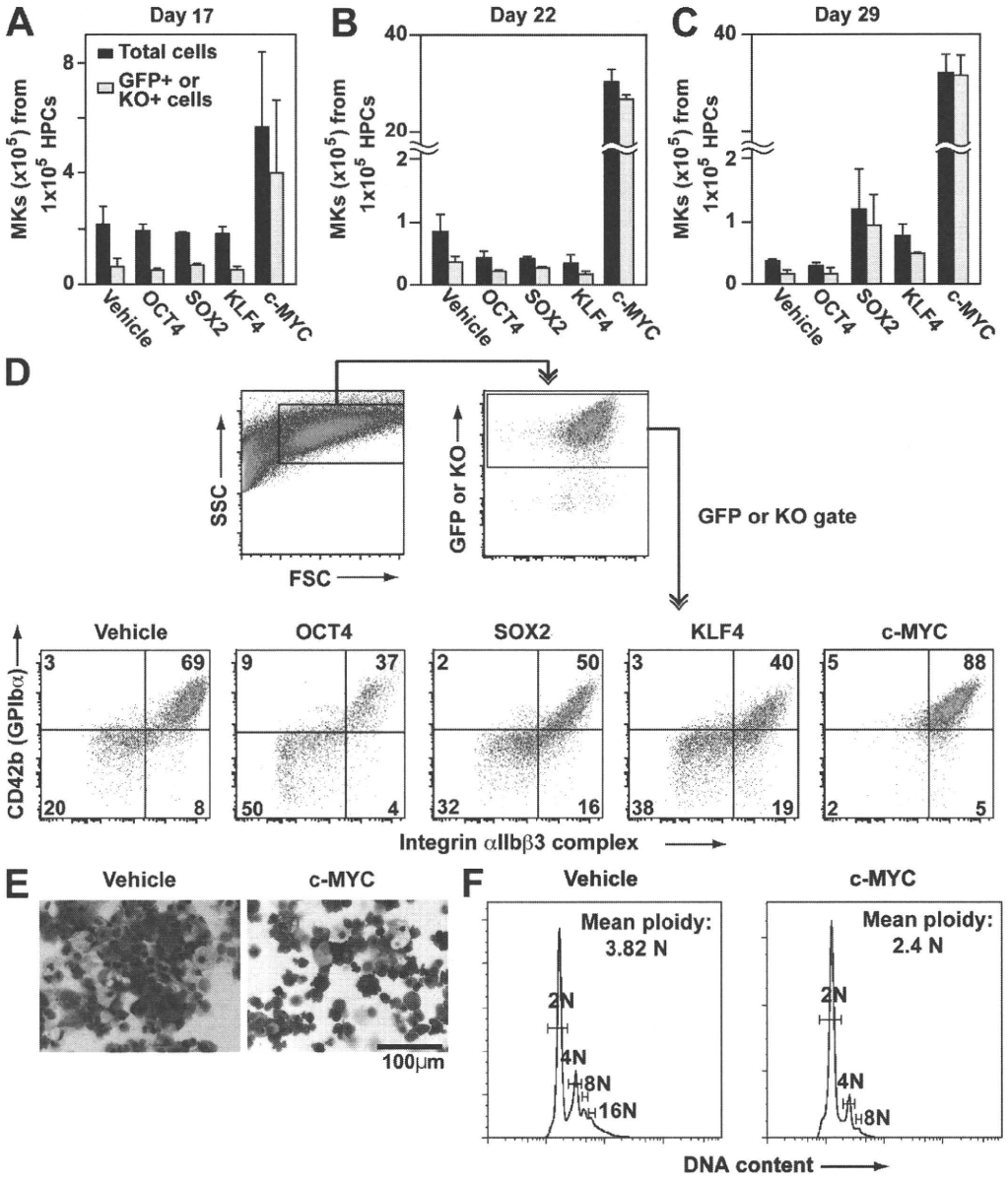

Figure 3. Effects of reprogramming factors on megakaryopoiesis. (A–C) Each reprogramming factor was transduced, together with EGFP or KO markers, on day 15 of MK-lineage culture. Numbers of total and marker genes EGFP or KO-expressing cells in floating cells on day 17 (A) and $CD42b^+$ MKs on days 22 (B) and 26 (C) were measured ($n = 3$, means ± SEM). (D) Representative flow cytometry dot plots of hESC-derived hematopoietic cells transduced with vehicle (EGFP), *OCT3/4-KO*, *SOX2-EGFP*, *KLF4-EGFP*, or *c-MYC-EGFP* on day 22. (E and F) On day 22, May-Giemsa staining (E) or ploidy analysis (F) of the cells transduced with vehicle or *c-MYC* was examined.

within iPS-Sacs, based on colony-forming capacity (Fig. S2 D) and their surface markers (not depicted). We found no significant differences between TkDA3-4 (four-factor) and TkDN4-M (three-factor; Fig. S2 D), which means the potential and the capacity to drive most myeloid lineage commitment from iPSC-derived progenitors is independent of the clone type, or at least there was no detectable difference between the three- and four-factor iPSC clones we examined (not depicted).

In contrast, quantitative (q) PCR analysis of hematopoietic cells on days 22–26 (7–11 d after replating for selective MK lineage culture) revealed expression of the exogenous (transgene [Tg]) reprogramming genes, which were not expressed before hematopoiesis (Fig. 2, A–D, day 0; and Fig. S1 B). Although qPCR after day 15 suggested that, in four-factor iPSCs, activation of *OCT3/4* Tg and/or *c-MYC* Tg might affect the enhanced megakaryopoiesis (Fig. 2, A and D), individual Tg activation was not dependent on the copy number in the genome (Fig. S1, D and E).

Thus, to confirm the functional effect of *OCT3/4* and/or *c-MYC* Tg on megakaryopoiesis from pluripotent stem cells,

Published November 22, 2010

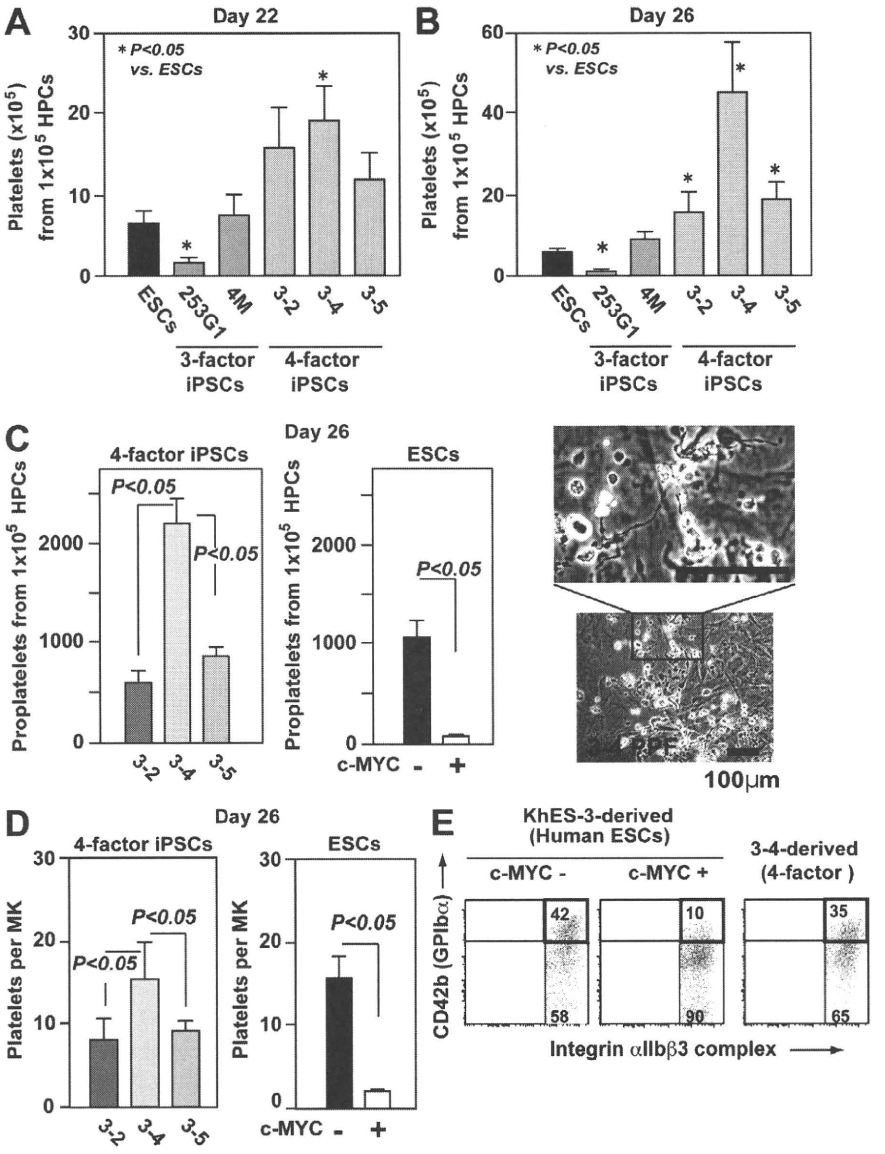

Figure 4. Level of *c-MYC* reactivation in individual iPSC-derived MKs may determine the efficiency of platelet generation in vitro. (A and B) Numbers of $CD41a^+CD42b^+$ platelets generated from hESCs or hiPSCs on days 22 (A) and 26 (B; peak of platelet generation; $n = 5$, means ± SEM). (C and D) Numbers of proplatelets (C) and platelets (D) derived from four-factor iPSCs and from ESC hematopoietic progenitors, with or without *c-MYC* transduction (ii; $n = 5$, means ± SEM). Representative photomicrographs of proplatelets are derived from four-factor iPSCs. (D) Numbers of platelets per MK was calculated as the total number of platelets divided by the total number of MKs on day 26 ($n = 5$, means ± SEM). (E) Representative flow cytometry dot plots show MKs derived from TkDA3-4 and KhES-3, with or without c-MYC transduction, on day 26.

each reprogramming factor was separately introduced into hematopoietic progenitors derived from KhES-3, along with EGFP or Kusabira orange (KO), which served as markers. Only *c-MYC* expression recapitulated the time course of the enhanced megakaryopoiesis, as it was accompanied by greater transduction efficiency as a result of the increased cell proliferation it induced (Fig. 3, A–C). Flow cytometry revealed that on day 22, most of the $EGFP^+$ or KO^+ population was $CD41a^+CD42b^+$ in the *c-MYC* O/E specimens but not in the others (Fig. 3 D), although only mononuclear and lower ploidy cells were present (Fig. 3, E and F). These suggest that *OCT3/4* O/E might not accelerate megakaryopoiesis (Fig. 3 D). Collectively then, these findings suggest that stronger expression of *c-MYC* in hESCs might promote lineage commitment into megakaryopoiesis without maturation.

c-MYC levels in hiPSC-derived MKs determines the number of platelets generated per MK

We next tested whether iPSC-derived MKs actually yield platelets in vitro. We confirmed that four-factor iPSCs generate greater numbers of platelets than three-factor iPSCs or hESCs (Fig. 4, A and B; and Fig. S5). Moreover, we noticed that, at the peak of production (day 26), many more proplatelets and platelets were generated from TkDA3-4 iPSCs than from any other four-factor iPSCs (Fig. 4, B and C; and Fig. S5). We also noted that TkDA3-2 and TkDA3-5 iPSC-derived MKs showed an earlier peak, on day 22 (Fig. 1, D and E; and Fig. S3) and that there were fewer proplatelets in the dishes (Fig. 4 C), which suggests that most MKs promote apoptosis and/or senescence leading to inhibition of platelet release in those two clones.

It has been reported that forced expression of *c-Myc* impairs maturation of MKs displaying polyploidization, leading to an increase in immature MKs (Thompson et al., 1996a). Indeed, we confirmed the appearance of immature MKs (Fig. 3, D–F) on day 22 after retroviral transduction of *c-MYC* into hESC-derived hematopoietic progenitors, which diminished proplatelet formation and platelet yield (Fig. 4, C and D; and Fig. S6 A). Dot plots for $CD41a^+CD42b^+$ platelets obtained by flow cytometric analysis of KhES-3, TkDN4-M (three-factor iPSCs), and TkDA3-4 (four-factor iPSCs) showed similar patterns (Fig. 4 E and Fig. S6 A), although most of the $CD41a^+CD42b^-$ platelets appeared to have shed the extracellular domain of

Published November 22, 2010

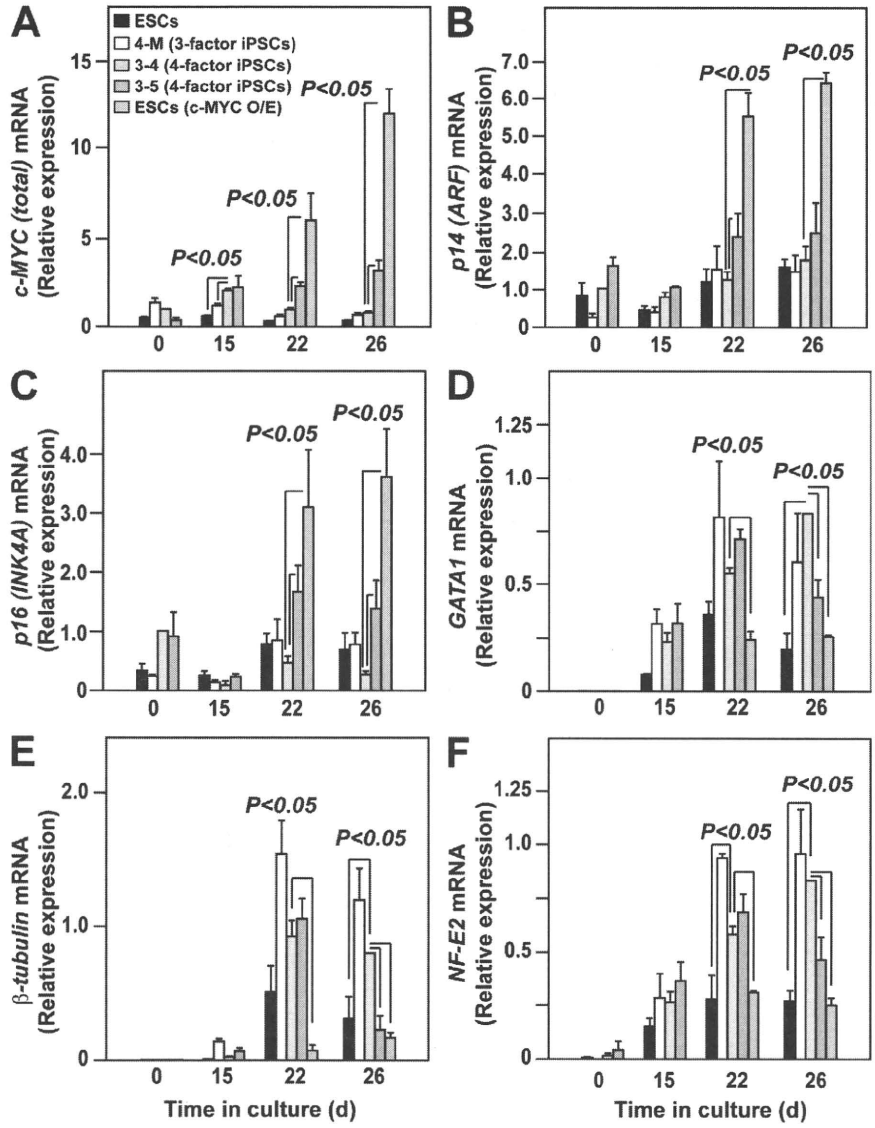

Figure 5. Level of *c-MYC* expression affects INK4A/ARF locus genes and genes related to MK maturation during megakaryopoiesis from pluripotent stem cells. qRT-PCR analysis of total *c-MYC* (A, endogenous plus exogenous), *p14ARF* (B), *p16INK4A* (C), *GATA1* (D), *β1-tubulin* (E), and *NF-E2 p45* (F) expression in hESCs, with and without overexpression (O/E) of exogenous *c-MYC*, on days 22 and 26 (7 and 11 d after transduction) in three-factor hiPSCs (TkDN4-M) or in four-factor hiPSCs (TkDA3-4 and TkDA3-5) on days 0, 15, 22, and 26. All levels were normalized to the level of *GAPDH* expression ($n = 4$ of two independent samples). The levels of *c-MYC* (A), *p14ARF* (B), *and p16INK4A* (C) expression in an undifferentiated TkDA3-4 iPSC clone (day 0) or expression of the other genes (D–F) in TkDA3-4–derived mature MKs (day 26) was assigned a value of 1.0 ($n = 4$, means ± SEM).

CD42b (GPIbα), as indicated by the recovery of CD42b expression in the presence of a metalloprotease inhibitor (Fig. S6 B; Nishikii et al., 2008). In contrast, platelet-like particles from hESC-derived MKs ectopically expressing *c-MYC* (*c-MYC*-O/E) showed significantly lower CD42b expression, a distinct pattern on dot plots (Fig. 4 E and Fig. S6 A), and no recovery of CD42b expression after administration of metalloprotease inhibitor (not depicted). Given the platelet generation per MK, it appears that forced expression of *c-MYC* in ESCs impairs platelet yield on day 26 (Fig. 4 D), which might recapitulate in TkDA3-2 or TkDA3-5 iPSC-MKs (Fig. 4 D).

How does the level of *c-MYC* expression control platelet generation from iPSCs?

The results so far suggest that excess *c-MYC* expression diminishes platelet yield. To confirm that hypothesis, we evaluated the time-dependent changes in the total expression of *c-MYC* and the genes involved in *c-MYC* activation and thrombopoiesis. qPCR analyses confirmed that total (endogenous plus exogenous) *c-MYC* expression in TkDA3-4, TkDA3-5, and *c-MYC*-O/E hESCs (KhES-3) was higher than in TkDN4-M (three-factor) or hESCs without *c-MYC* (control) on days 15 (hematopoietic progenitors) and 22 (immature MKs) of culture (Fig. 5 A). Intriguingly, however, total *c-MYC* expression in TkDA3-5 increased progressively from days 15 through 26, whereas in TkDA3-4, the iPSC clone showing the most efficient platelet generation, total *c-MYC* expression declined after day 15 (Fig. 5 A). To confirm whether reactivation actually influenced total c-MYC expression (Fig. 5 A), we separately examined endogenous and exogenous (Tg) *c-MYC* expression. We found that although levels of total and exogenous *c-MYC* differed among the clones (Fig. 5 A and Fig. S7 A), there was no significant difference in endogenous c-MYC levels among TkDN4-M, TkDA3-4, and TkDA3-5 (Fig. S7 B). In contrast, expression of two INK4A locus genes, *p14* (*ARF*) and *p16* (*INK4A*), which act as a safety net system against *c-Myc* hyperactivation leading to senescence (Murphy et al., 2008), was higher in *c-MYC*-O/E hESCs and TkDA3-5 than in TkDA3-4 on day 22 (immature MKs; Fig. 5, B and C). We therefore assumed that elevation of *p14* and *p16*, beginning at an earlier phase of differentiation, is associated with inhibition of MK maturation (Fig. 3, E and F). MYC associates with the GATA1 promoter during immature erythroblast expansion, perhaps suppressing GATA-1 expression (Rylski et al., 2003). Similarly,

Published November 22, 2010

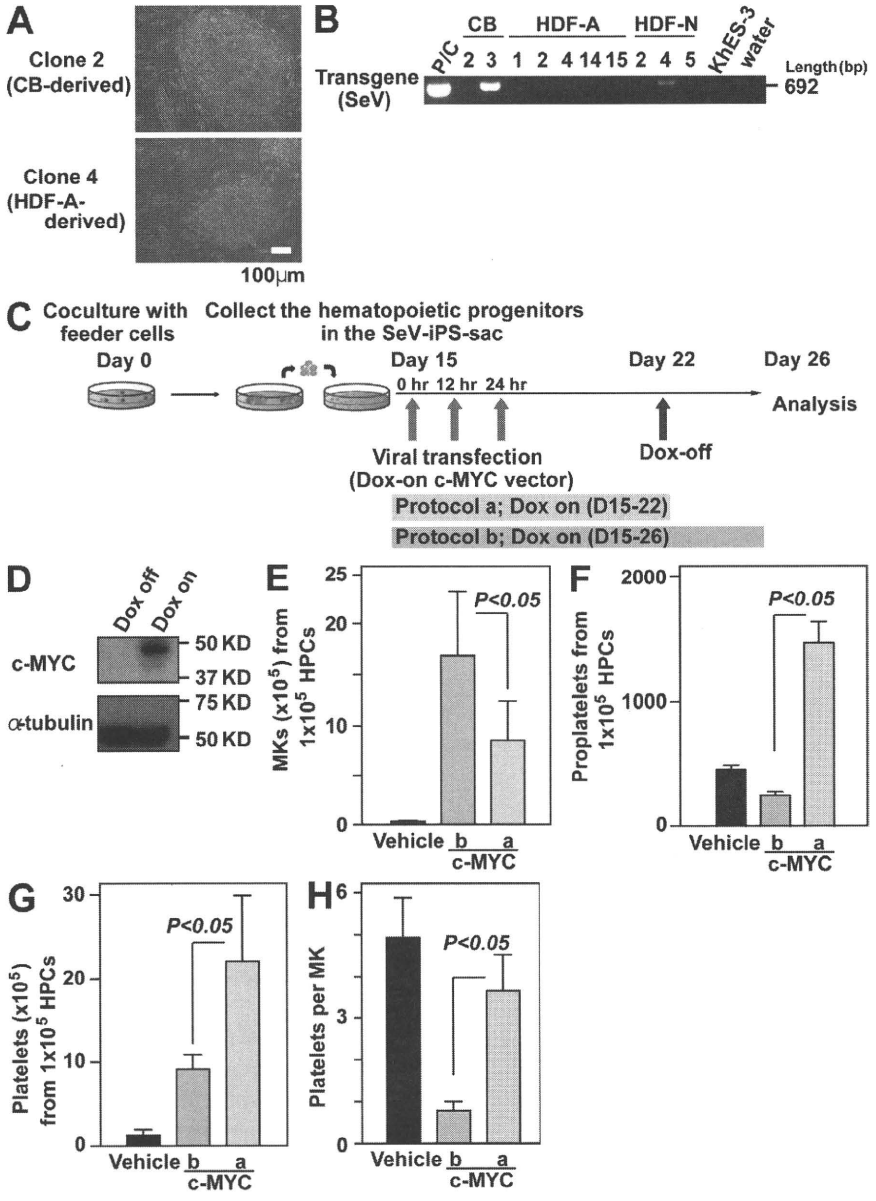

Figure 6. Inducible c-MYC expression system enabling Sendai viral vector–based iPSCs without reactivation to recapitulate enhanced MK maturation with increased platelet generation. (A) Representative photomicrographs of SeV-iPSCs derived from CB $CD34^+CD45^+$ cells or HDFs. Original magnification, 100×. (B) RT-PCR analyses of Sendai virus Tg (harboring reprogramming factors) expression in SeV-iPSC clones (passage number 4) derived from CB, HDF-A (adult), and HDF-N (neonate). A sample of HDFs transduced with SeV is used as a positive control for the SeV Tg. (C) Scheme of *c-MYC* induction in SeV-iPSC-derived hematopoietic cells. Hematopoietic progenitors derived from SeV-iPSCs were transfected with DOX-inducible *c-MYC* O/E vector on day 15 and analyzed on day 26. In Protocol a, DOX was added only from days 15 to 22. In protocol b, DOX was added from days 15 through 26. (D) Representative Western blots of cell lysates with *c-MYC* O/E (DOX-on; protocol b) or without *c-MYC* O/E (DOX-off; Protocol a) on day 26. The α-tubulin levels indicate same protein value. (E–G) Numbers of CD42b $(GPIb\alpha)^+$ MKs (E), proplatelets (F), and platelets (G) on day 26 derived from 10^5 hematopoietic progenitors transfected with vehicle or DOX-inducible c-MYC O/E vector in protocol a or protocol b ($n = 4$, means ± SEM). (H) Numbers of platelets per MK generated on day 26 of culture (peak of platelet generation; $n = 4$, means ± SEM). Numbers of platelets per MK were calculated as the total number of platelets divided by the total number of MKs on day 26.

GATA-1 expression was reduced in *c-MYC*-O/E hESC (KhES-3)-MKs showing higher levels of *c-MYC* expression on day 22, as were levels of *β1-tublin* and *NF-E2* (*p45*; Fig. 5, D–F). Consistent with those findings, both *c-MYC*-O/E MKs and TkDA3-5–derived MKs showed less proplatelet formation (Fig. 4 C) and had a smaller platelet yield than TkDA3-4 (Fig. 4 D). Thus, high levels of sustained expression of *INK4A* locus genes in MKs are also associated with impaired platelet release.

These results suggest that an increase in *c-MYC* expression, peaking on day 22, followed by a decline may be critical for efficient platelet generation on day 26, as exemplified in TkDA3-4. Sustained increases in *c-MYC* expression may contribute to activation of senescence genes, thereby impairing MK maturation and intact platelet yield.

Inducible *c-MYC* expression in iPSCs without reactivation exhibited behavior similar to that of iPSCs with reactivation, leading to efficient generation of functional platelets

To further confirm whether an increase and subsequent decline in c-MYC is critical for megakaryopoiesis, leading to an efficient platelet yield, we prepared a Sendai viral vector (SeV) harboring the four reprogramming genes, which, during the generation of human iPSCs, enabled RNA viral transduction without integration of DNA into the chromosome (Nishimura et al., 2007; Fig. 6, A and B). Thereafter, doxycycline (DOX)-inducible expression system in a lentiviral vector was applied to the SeV-based human iPSCs (SeV-iPSCs; skin-fibroblast [HDF]-derived SeV-iPSCs and cord blood [CB] $CD34^+$ cell-derived SeV-iPSCs; Fig. 6 A). We selected CB-derived SeV-iPSCs (clone 2; Fig. 6, A and B) for most experiments because they showed no detectable Tg and better differentiation to hematopoietic progenitors than other clones, including HDF-derived SeV-iPSCs (not depicted). *c-MYC* O/E was regulated by DOX (Fig. 6 C), and

Published November 22, 2010

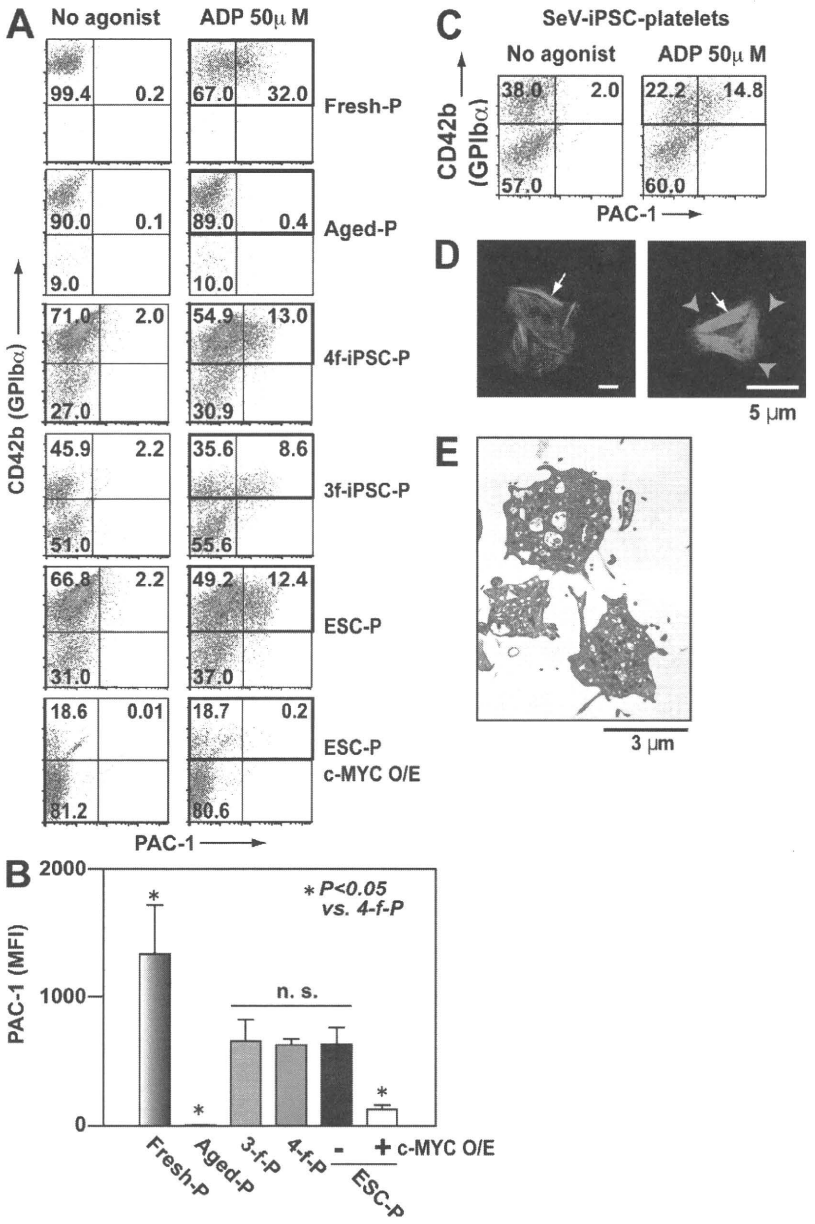

Figure 7. Integrin activation and the structure of human iPSC platelets are comparable to those in human PB-derived platelets. (A–C) Integrin activation in fresh human platelets (Fresh-P), aged human platelets (48-h incubation at 37°C; Aged-P), TkDN4-M (three-factor iPSC) platelets (3f-iPSC-P), TkDA3-4 (four-factor iPSC) platelets (4f-iPSC-P), and ESC platelets (ESC-P), with or without *c-MYC* O/E. The binding of PAC-1 (indicative of platelet activation) to individual platelets was quantified in the absence and presence of 50 μM ADP using flow cytometry. (A) Representative flow cytometry dot plots. Square indicates $CD42b^+$ platelets. (B) Mean fluorescence intensity (MFI) of bound PAC-1, obtained from square gate in A. Error bars depict means ± SEM for four independent experiments (duplicate). (C) Representative flow cytometry analysis of PAC-1–bound platelets generated from integration-free SeV-iPSCs subjected to biphasic activation and, thereafter, decline of c-MYC expression as protocol b shown in Fig. 6 C. Square indicates $CD42b^+$ platelets. (D) Spreading of iPSC platelets on fibrinogen. Human CD41a (red) and phalloidin (green) were used to identify F-actin fibers. Arrowheads indicate lamellipodia. Arrows indicate actin stress fibers. Bars, 5 μm. (E) Transmission electron micrographs of hiPSC (TkDA3-4) platelets on day 26. Bar, 3 μm.

we confirmed that day 22 was the most suitable point to turn off O/E. The results also showed that continuous *c-MYC* O/E from days 22 to 26 still increased the number of MKs (Fig. 6 E), whereas the lack of *c-MYC* O/E from days 22 to 26 increased the total numbers of proplatelets (Fig. 6 F) or $CD41a^+CD42b^+$ platelets (Fig. 6 G). An increase in platelet yield per MK was also evident with the absence of *c-MYC* O/E after day 22 (Fig. 6 H), confirming the effect of *c-MYC* expression on megakaryopoiesis.

Human iPSC-derived platelets function normally in vitro and in vivo

To assess the effect of *c-MYC* reactivation on the functionality of platelets from TkDA3-4, we compared agonist-induced integrin activation in human platelets (from peripheral blood [PB]), PB-based aged platelets (48-h incubation; Bergmeier et al., 2003; Nishikii et al., 2008), iPSC platelets, and ESC platelets. The aged platelets were tested because iPSC-derived platelets were heterogeneously produced from MKs at various stages in culture, so that many of the platelets produced could have become aged (Nishikii et al., 2008). Conformational changes in integrins are required for platelet aggregation and stable thrombosis in vivo (Shattil et al., 1985). Indeed, although PB-based aged platelets were nonresponders, the integrin activity of TkDA3-4 (four-factor iPSCs) platelets was comparable to that of TkDN4-M (three-factor iPSCs) platelets, which showed a weaker response than human PB platelets (Fig. 7, A and B; and Fig. S8 A). Notably, *c-MYC* O/E-dependent iPSC-derived platelets showed little binding (Fig. 7, A and B). In contrast, platelets produced from SeV-iPSCs-MKs in the absence of *c-MYC* O/E after its activation responded well to ADP stimulation (Fig. 7 C). We therefore conclude that *c-MYC* activation and decline during MK differentiation may lead to the generation of functional platelets from iPSCs. We also examined expression of P-selectin (CD62P) on platelets in the presence of 50 μM ADP and observed weak but positive P-selectin expression in iPSC-derived platelets (Fig. S8 B).

Published November 22, 2010

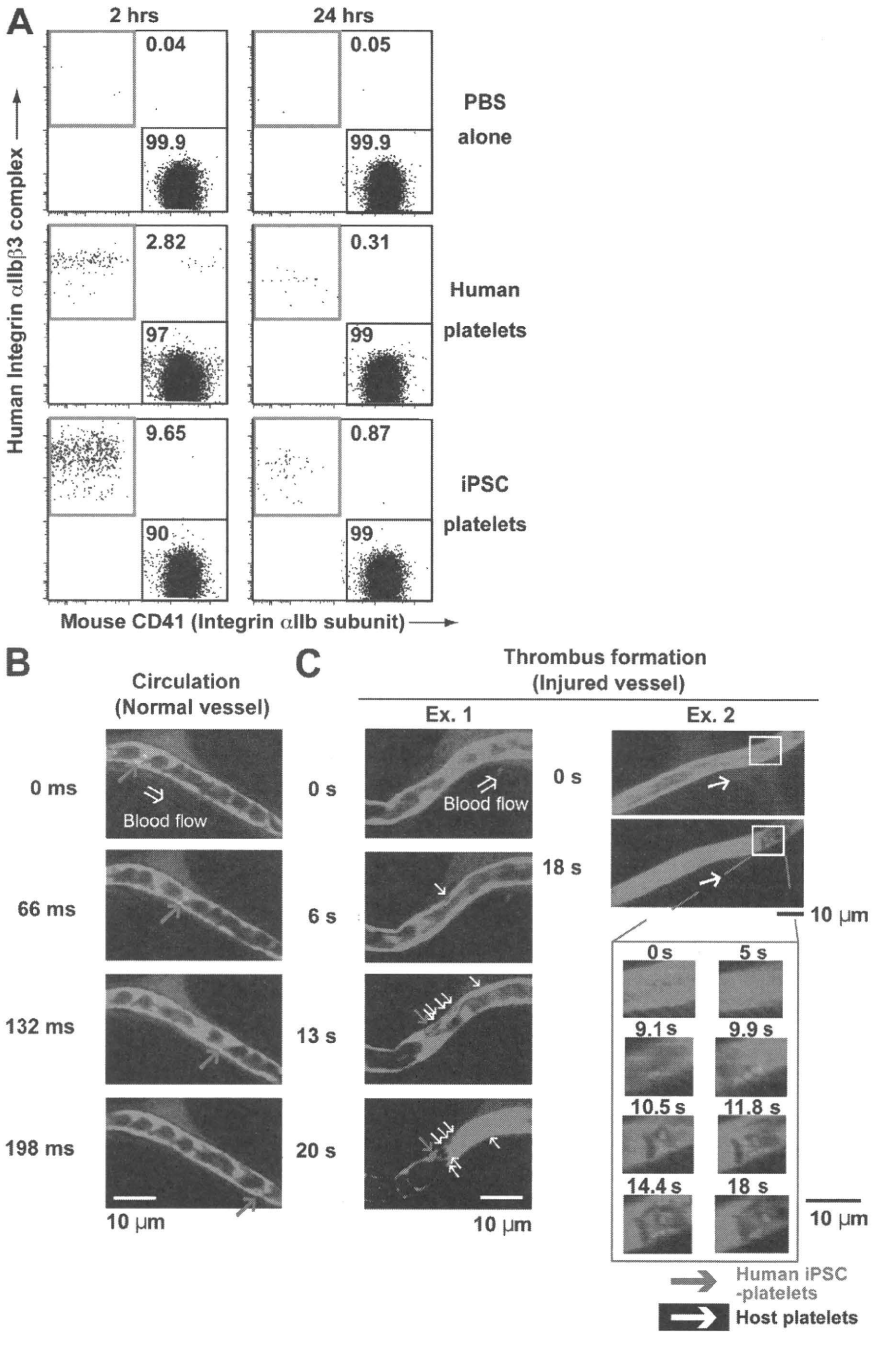

Figure 8. Human iPSC platelets circulate in NOG mice and adhere to vessel during thrombus formation in vivo. (A) NOG (nod-scid/IL-2 γc-null) mice were irradiated (2.0 Gy) to induce thrombocytopenia. 9 d later, human iPSC platelets, human PB-derived platelets (10^7), or PBS alone was injected via the tail vein. Platelet chimerism was quantified by flow cytometry. Representative dot plots for the same experiment are shown. Circulation of injected platelets was evaluated after 2 and 24 h (orange squares). Experiments were independently performed three times. (B) Sequential images of circulating iPSC platelets. A combination of FITC-dextran (green) and 10^7 TMRE-stained iPSC platelets (red) in PBS was injected via the tail vein into NOG mice. Mesenteric capillaries were visualized using a confocal laser-scanning microscope. Red arrows indicate circulating iPSC platelets in vivo. Original videos are available as Video 2. (C) Representative sequential images of thrombus formation by iPSC platelets in a blood vessel. Hematoporphyrin was administrated to induce thrombus formation after laser-induced injury, as described previously (Nishimura et al., 2008; Takizawa et al., 2010). Red arrows indicate iPSC platelets in a developing thrombus. White arrows indicate host (mouse) platelets. Original videos are available as Videos 3–5. Experiments were independently performed three times. Bars, 10 μm.

TkDA3-4 iPSC platelets on immobilized fibrinogen exhibited filopodia, lamellipodia, and/or actin stress fibers, all of which are also indicative of platelet thrombosis (Shattil et al., 1985; Fig. 7 D), suggesting that appropriate elevation and then reduction of *c-MYC* expression increases production efficiency without impairing platelet functionality, at least in vitro. Moreover, the granule content and structural components of TkDA3-4 iPSC platelets appeared normal when examined under transmission electron microscopy (Fig. 7 E), which implies a capacity for hemostasis in vivo.

In contrast, as in the previous paragraph, we recently showed that culture at 37°C influences the degradation of platelets by causing them to shed the extracellular domain of GPIbα, which is required for initial adhesion to the injured vessel wall (Nishikii et al., 2008; Fig. S6 B). In vivo, platelets lacking the GPIbα extracellular domain are quickly cleared from the circulation (Bergmeier et al., 2003), leading to insufficient levels of circulating platelets after transfusion (Nishikii et al., 2008). To avoid this without affecting platelet yield, we applied GM6001, a nonspecific inhibitor to metalloproteases, for 2 d before collection of cultured platelets and confirmed that the shedding of GPIbα was dose-dependently inhibited by GM6001 (Fig. S6 B; Nishikii et al., 2008).

We next sought to develop a transfusion model to assess platelet circulation in vivo. Using a NOG (nod-scid/IL-2 γc-null) mouse thrombocytopenia model induced by irradiation (2.0 Gy, 9 d beforehand), flow cytometric analyses performed

Published November 22, 2010

2 and 24 h after transfusion (~1.0–1.2 × 10^7 platelets/mouse) showed that four-factor iPSC platelets were consistently present and that the percentage circulating was similar to that obtained with fresh human platelets (platelet chimerism of human CD41a$^+$/mouse CD41a$^+$; 3–10%, 2 h after transfusion; Fig. 8 A).

To further assess and confirm the functionality of TkDA3-4 hiPSC platelets in vivo, we used the same NOG mouse model (Fig. 8 A) with high–spatiotemporal resolution confocal laser microscopy to visualize the behavior of individual platelets upon initiation of adhesion to an injured vessel wall and during the subsequent steps in thrombus formation under flow within the vessel (Takizawa et al., 2010). iPSC platelets stained with tetramethylrhodamine ethyl ester, which is incorporated into the external lipid layer of the cell membrane, were transfused into NOG mice (2 Gy, 14 d beforehand), after which we confirmed they circulated as individual platelets (Fig. 8 B, red; and Video 2). Then using our novel laser injury thrombus model (Takizawa et al., 2010), we clearly observed that iPSC platelets initially adhered to the injured vessel wall, coordinating with host platelets and ultimately leading to thrombus formation and vessel occlusion (Fig. 8 C; and Videos 3–5). Thus, four-factor iPSC platelets appear capable of mediating hemostasis and thrombosis in vivo.

DISCUSSION

Megakaryocytic lineage-restricted *c-Myc* expression in mouse models showed this gene to be a positive regulator of MK progenitor proliferation (Thompson et al., 1996a,b) and to be required for TPO/c-mpl signaling in megakaryopoiesis (Chanprasert et al., 2006). Notably, *c-Myc* deficiency also accelerates megakaryopoiesis, but with lower ploidy (up to 8n), and augments immature platelet release accompanied by an increase in the platelet count. In our hiPSC culture system, however, total cellular *c-MYC* expression (endogenous plus reactivation of exogenous) appeared to be at an appropriate, and probably restricted, level suitable for promoting platelet generation (Fig. 4 B, Fig. 5 A, and Fig. 6 G, day 26). Increasing MYC levels enables cells to move from quiescence to S phase, even in the absence of mitogens (Eilers et al., 1991), possibly through activation of target genes (*cyclin D1(D2,D3)/Cdk4(6)* and *cyclin E/Cdk2*). In that regard, although MYC activity, per se, is required for normal cell proliferation (Murphy et al., 2008), it is recognized that above a certain threshold *c-Myc* expression may induce the onset of oncogenesis. Moreover, excessively high MYC levels induce senescence via activation of the Arf–Mdm2–p53 pathway (Eischen et al., 1999; Murphy et al., 2008) and suppression of key regulators of MK maturation, such as GATA1, β1-tubulin, and NFE2, which likely inhibits maturation (Fig. 5, B–F) and may also induce apoptosis in some cells (Askew et al., 1991; Evan et al., 1992).

Four-factor hiPSC-derived hematopoietic progenitors also generate much larger numbers of platelets than three-factor iPSCs or hESCs (Fig. 4, A and B; and Fig. S5), possibly as a result of MK proliferation mediated though *c-MYC* reactivation (Fig. 3 A; Fig. 4, A and B; and Fig. S3). However, the number of platelets per MK derived from individual four-factor hiPSC clones (TkDA3-2, -4, and –5; with *c-MYC*) and ESCs (with or without *c-MYC*) on day 26 differs (Fig. 4 D). Nonetheless, TkDA3-4, which is the most efficient platelet-producing clone (Fig. 4, B and D; and Fig. S5), shows weaker *c-MYC* expression than other four-factor iPSCs or *c-MYC*-O/E MKs (Fig. 5 A). Indeed, DOX-inducible expression of *c-MYC* O/E in genome integration-free iPSCs (SeV-iPSCs) confirmed our hypothesis (Fig. 6, A–H). In addition, when we considered the possibility that deregulated MK maturation leads to release of nonfunctional platelets, we found differences in platelet functionality between hESCs or SeV-iPSCs, with or without *c-MYC*, and iPSC clones (Fig. 7, A–C). Immature megakaryocytic cell lines, such as Meg01, are reportedly capable of releasing CD41a$^+$ platelet-like particles, but they show poor functionality in vitro (Takeuchi et al., 1998). We also found that hESC-derived CD41$^+$ particles showed significantly less CD42b expression when *c-MYC* was ectopically expressed in MKs (Fig. 4 E and Fig. S6 A) and showed poor functionality in vitro (Fig. 7, A and B). In contrast, the function of CD42b$^+$ platelets generated from TkDA3-4 was intact and able to mediate hemostasis in vivo, although some of the yield was likely made up of nonfunctional aged platelets (Fig. 7 and Fig. 8 C).

To clarify the underlying mechanism, we examined the association between platelet generation and gene expression. In *c-MYC*-O/E MKs, expression of *GATA1* (Vyas et al., 1999; Rylski et al., 2003), a key regulator for MK maturation and polyploidization, was suppressed, whereas *INK4A* and *ARF* expression was greatly up-regulated (Fig. 5, B–D; Eischen et al., 1999; Murphy et al., 2008). Consequently, the maturation phase was inhibited, as exemplified by the presence of hypoploid cells without proplatelets (Fig. 3, E and F; and Fig. 4 C) and the weak expression of mature MK markers *β1-tubulin* and *NF-E2* (Fig. 5, E and F), as well as *platelet factor 4* (not depicted; Patel et al., 2005; Schulze and Shivdasani, 2005). These MKs only generated a few nonfunctional CD41a$^+$CD42b$^+$ platelets (Fig. 4, D and E; Fig. 5 A; and Fig. 7 B). In contrast, MKs derived from TkDA3-4 transiently showed appropriately high levels of *c-MYC* expression, with no effect on expression of *INK4A/ARF* locus genes (Fig. 5, A [day 15], B, and C), after which *c-MYC* expression declined (Fig. 5 A, days 22 and 26). From days 22 to 26, the pattern of *GATA1*, *β1-tubulin*, and *NF-E2* expression was opposite that of *c-MYC* expression (Fig. 5, D–F), indicating that reduction of *c-MYC* after day 22 (immature MKs) may be required for MK maturation and generation of functional platelets (e.g., day 26). We therefore suppose that because most MKs derived from TkDA3-5, which produced fewer platelets than TkDA3-4 (Fig. 4 D), showed sustained *c-MYC* activity, leading to up-regulation of *INK4A/ARF* locus genes (Fig. 5), those MKs were unable to complete the maturation phase, even though *GATA-1*, *β1-tubulin*, and *NF-E2* expression was enhanced (Fig. 5, D–F). We further confirmed this phenomenon using integration-free SeV-iPSCs in a DOX-inducible gene expression system. Removal of *c-MYC* O/E from day 22 until day 26 increased the total numbers of proplatelets (Fig. 6 F) and

Published November 22, 2010

$CD42b^+$ functional platelets (Fig. 6 G and Fig. 7 C), as compared with the numbers seen with continuous *c-MYC* O/E until day 26. We therefore conclude that increased expression of *c-MYC* in hematopoietic progenitors may promote megakaryopoiesis, leading to increased MK generation (Fig. 6 E), but that a sustained increase in *c-MYC* after the MK progenitor stage may impair MK maturation, thereby diminishing platelet release (Fig. 6, F and G).

Both hESCs and hiPSCs were previously shown to differentiate into hematopoietic cells (Wang et al., 2004; Vodyanik et al., 2005; Ma et al., 2008; Choi et al., 2009; Yokoyama et al., 2009), although with the exception of hESC-derived natural killer cells (Woll et al., 2009), only in vitro functionality has been reported. In this paper, we demonstrated that platelets derived from hiPSCs via a mechanism involving limited *c-MYC* reactivation (Fig. 4 B and Fig. 5 A) are capable of thrombus formation in vivo.

Recent studies suggest that the source of the somatic cells and introduction of reprogramming factors without *c-Myc* (retroviral vectors, plasmids, proteins, Sendai viral vectors, and so on), also known as *L-Myc/L-MYC*, are essential elements for selection of efficient and safe iPSC clones (Okita et al., 2007; Nakagawa et al., 2010). We propose that selection of the iPSC clones most suitable for their purpose should also be considered. Our analysis of multiple hiPSC clones accompanied by Tg genome integration or a DOX-inducible expression system shows that time-dependent changes in *c-MYC* expression, specifically up-regulation and then down-regulation within an appropriate time span, facilitates generation of a novel platelet transfusion system derived from hiPSCs. It is noteworthy that in vitro generation of platelet concentrates custom made from HLA-identical donors or the patients themselves are not subject to immune rejection and do not require donor blood. We propose that iPSC platelets could be an invaluable resource for patients requiring repeated platelet transfusion and that this system should enable us to investigate as yet unresolved aspects of the mechanisms underlying thrombocytopenia.

MATERIALS AND METHODS

Cells, reagents, viral vectors, and mice. All reagents were obtained from Sigma-Aldrich unless indicated otherwise. The human ESC clone Kyoto hESCs (KhES) 3 was obtained from the Institute for Frontier Medical Science, Kyoto University (Kyoto, Japan) after approval for hESC use was granted by the Minister of Education, Culture, Sports, Science, and Technology of Japan. PB was provided from healthy volunteers approved by ethical committee of the Institute of Medical Science at University of Tokyo for human sample-based experiments. The entire study using human samples was conducted in accordance with the Declaration of Helsinki. Animal experiments and use of viral vectors were approved by the committees of the Institute of Medical Science and School of Medicine at University of Tokyo. pMX retroviral vectors were from T. Kitanura (The University of Tokyo, Tokyo, Japan). Original hiPSC clones, 201B6, 201B7, 253G1, and 253G4 (Kyoto University), were used as a reference (Takahashi et al., 2007). We established other hiPSC clones derived from HDFs (Cell Applications, Inc.) using a retrovirus harboring four (*OCT3/4, SOX2, KLF4,* and *c-MYC*) or three (without *c-MYC*) reprogramming factors: TkDA3-1, -2, -4, -5, -9, and -20 and TkDN4-M clones. HDFs were cultivated in DME supplemented with 10% FBS, 2 mM L-glutamine, 100 U/ml penicillin, and 0.1 mg/ml streptomycin. All pluripotent cells were maintained as described previously (Takahashi et al., 2007). The mouse C3H10T1/2 cell line was purchased from the Institute of Physical and Chemical Research Bio-Resource Center (Tsukuba, Ibaraki, Japan) and was cultured as described previously (Takayama et al., 2008). Retroviral supernatants for establishing iPSCs were obtained from a 293 GPG system (provided by R.C. Mulligan, Children's Hospital Boston, Boston, MA; Ory et al., 1996). SeV vector harboring human *OCT3/4, SOX2, KLF4,* and *c-MYC* was based upon original SeV vector and viral supernatants were made as previously described (Nishimura et al., 2007). Another set of hiPSCs without genome integration was established using SeV harboring four factors from HDFs or CB $CD34^+/CD45^+$ cells (Lonza). Hematopoietic differentiation from iPSCs and hESCs was performed in the same medium, as described previously (Takayama et al., 2008). The following antibodies were used: PE-conjugated anti-CD9, PE-conjugated anti-CD31, PE- or FITC-conjugated anti-CD34, unconjugated or allophycocyanin (APC)-conjugated anti-CD41a (HIP8 clone), FITC-conjugated anti-CD42a, PE-conjugated anti-CD42b, Alexa Fluor 405–conjugated anti-CD45, and APC-conjugated anti–VEGF-R2. FITC-conjugated PAC-1 (BD) and FITC-conjugated anti-CD62P (P-selectin; BioLegend) antibodies were used for platelet activation studies (Shattil et al., 1985). Tirofiban (Takayama et al., 2008), a specific antagonist of human integrin $\alpha IIb\beta 3$, was obtained from Merck. Anti–c-Myc (1:400; Santa Cruz Biotechnology, Inc.), anti–α-tubulin (1:1,000; Sigma-Aldrich), anti–mouse IgG-HRP (1:5,000; GE Healthcare), and anti–rabbit IgG-HRP (1:2,500; GE Healthcare) antibodies were used for Western blotting. 15-wk-old NOG mice were obtained from the Central Institute for Experimental Animals (Kanagawa, Japan) and were maintained under specific pathogen-free conditions. The mice were irradiated at 2.0 Gy to induce thrombocytopenia and have analyzed for platelet chimerism using an Aria flow cytometer (BD) or by in vivo imaging using a confocal laser-scanning microscope (CSU-X1; Yokogawa Electronics).

Induction of human iPSCs using high-titer retroviruses or SeV viruses. hiPSCs were established from HDFs using high-titer retroviruses derived from 293GPG cells (Ory et al., 1996). Integration-free human iPSCs were established with SeV harboring human *OCT3/4, SOX2, KLF4,* and *c-MYC* as described in the previous section. CB cells were infected with SeV in the same basal medium (Takayama et al., 2008) supplemented with 50 ng/ml human SCF (R&D Systems), human TPO (R&D Systems), and human FMS-related tyrosine kinase 3 ligand (FLT3-L; PeproTech).

Immunohistochemistry of human ESCs and human iPSCs. hiPSCs were fixed with 4% paraformaldehyde in PBS, after which they were labeled first with an antibody against human SSEA4 (Millipore) and then with a secondary antibody and observed using an epifluorescence microscope (DM IRBE; Leica).

Semi-qRT-PCR. hiPSCs were lysed with Trizol (Invitrogen), after which total RNA was extracted as recommended by the manufacturer. Complementary DNAs were obtained using an RT-PCR System (Thermo Fisher Scientific) and oligo-dT primers (Invitrogen). Samples were normalized to intrinsic *GAPDH*. Semi-qRT-PCR was performed to determine the expression levels of genes of interest. Amplification proceeded for 26–32 cycles. The primer sets used are shown in Table S1.

Teratoma formation and histological analysis. hiPSCs were prepared from 10^7 cells/ml in PBS. Male NOD/Scid mice were anesthetized with diethyl ether, after which aliquots of suspended cells ($1–3 \times 10^6$ cells) were injected into their testes. 8 wk after injection, the mice were sacrificed, and the resultant tumors were dissected. Tumor samples were then fixed in 4% paraformaldehyde, embedded in paraffin, sectioned, and stained with hematoxylin and eosin.

Southern blotting analysis. 7 μg of genomic DNA was digested with BglII, EcoRI, and NcoI or NaeI, NdeI, and NcoI for c-MYC or Oct3/4, respectively, overnight. Digested DNA fragments were separated on 0.8% agarose gel and transferred to a nylon membrane (GE Healthcare). The membranes were

Published November 22, 2010

hybridized with radioactively labeled DNA probes (c-MYC-exon3 or Oct3/4-exon1) in PerfectHyb Plus Hybridization buffer (Sigma-Aldrich) at 55°C overnight with constant agitation. After washing, signals were detected by the FLA-5100 imaging system (Fujifilm).

Hematopoietic differentiation of hiPSCs. To differentiate hiPSCs into hematopoietic cells, we used the same protocol we established with hESCs (Takayama et al., 2008). In brief, small clumps of hiPSCs (<100 cells treated with PBS containing 0.25% trypsin, 1 mM $CaCl_2$, and 20% KSR) were transferred onto irradiated C3H10T1/2 cells and co-cultured in hematopoietic cell differentiation medium, which was refreshed every 3 d. On days 14–15 of culture, the iPS-Sacs were collected into a 50-ml tube, gently crushed with a pipette and passed through a 40-μm cell strainer to obtain hematopoietic progenitors, which were transferred onto freshly irradiated feeder cells and cultured in differentiation medium established as previously in human ESCs (Takayama et al., 2008). The medium was refreshed every 3 d, and nonadherent cells were collected and analyzed from days 22 to 38.

DOX-inducible c-MYC lentiviral vector. The *c-MYC* gene-inducible lentiviral vector was based upon LV-TRE-mOKS-Ubc-rTA-I2G (Kobayashi et al., 2010) and made by replacing the mOKS cassette with *c-MYC* gene. Viral supernatant was generated as previously described (Eto et al., 2007).

Western blotting analysis. Experiments were performed as previously described (Eto et al., 2007; Nishikii et al., 2008). In brief, 45 μg of cell lysates treated with TNE buffer (10 mM Tris-HCl, pH 7.8, 150 mM NaCl, 1% NP-40, and 1 mM EDTA), supplemented with protease inhibitor cocktail (Roche), were separated by electrophoresis on 10–20% SDS-polyacrylamide gradient gel (Bio-Rad Laboratories) and transferred to a polyvinylidine difluoride membrane (Millipore), followed by visualization with SuperSignal West Pico Chemiluminescent Substrate (Thermo Fisher Scientific).

Immunohistochemical and flow cytometric analyses of ES- and iPS-Sacs. Immunohistochemical staining of iPS-Sacs was performed on day 14 or 15. Intact iPS-Sacs were fixed with 10% methanol in PBS, after which they were stained first with an antibody against human VEGF-R2 and then with a secondary antibody and observed using an epifluorescence microscope (DM IRBE; Leica). Round cells within the ES- and iPS-Sacs were stained with anti–human CD31-PE, CD34-FITC, CD38-APC, CD41a-APC, CD45–Alexa Fluor 405, or VEGF-R2–APC antibodies and analyzed by flow cytometry.

Hematopoietic colony-forming cell assay. Hematopoietic colony-forming cell assays were performed in MethoCult H4434 semisolid medium (STEMCELL Technologies Inc.) supplemented with 50 ng/ml human TPO. 10,000 hematopoietic progenitors from within an iPS-Sac were plated in 1.5 ml of medium and cultivated for 14 d. The colonies were then collected, stained with Hemacolor (Merck), and observed under a microscope.

Flow cytometric analysis of MKs. Nonadherent cells on days 22–38 were prepared in PBS containing 2% FBS and stained with combinations of antibodies for 30 min on ice. Samples were then washed with PBS and analyzed by flow cytometry (FACSAria; BD).

Viral transduction of hematopoietic progenitors within ES-sacs. A total of 10^5 hematopoietic progenitors harvested from within an ES-sac or iPS-sac on day 15 of culture were suspended in hematopoietic differentiation medium containing 50 ng/ml of human SCF, 100 ng/ml of human TPO, 25 U/ml heparin, and 10 mg/ml protamine sulfate and then transduced with viral supernatant for vehicle, *OCT3/4-KO*, *SOX2-EGFP*, *KLF4-EGFP*, *c-MYC-EGFP*, or DOX-inducible *c-MYC*. The cells were then replated into a 6-well plate precoated with C3H10T1/2 cells and centrifuged at 900 rpm for 60 min at 32°C. The viral transduction was performed three times with 12-h intervals in between. To induce *c-MYC* O/E, 1 μg/ml DOX was added to the culture medium from days 15 to 22 or 26 (Fig. 5 C).

qRT-PCR. cDNA samples were prepared as described in the previous section. Real-time PCR was performed using a kit (TaqMan Gene Expression Master Mix [Applied Biosystems] or SYBR Premix Dimer Eraser [Takara Bio, Inc.]) according to the manufacturer's instructions. Signals were detected using an ABI7900HT Real-Time PCR System (Applied Biosystems). Primer sets for *GAPDH*, *c-MYC*, *p14ARF*, *p16INK4A*, *GATA-1*, *β1-tubulin*, and *NF-E2 p45* were determined using the Universal Probe Library Set for humans (https://www.roche-applied-science.com/sis/rtpcr/upl/index.jsp?id=UP030000). Primer sets for exogenous OCT3/4, SOX2, KLF4, c-MYC, and endogenous c-MYC are listed in Table S1.

Electron microscopic observation of hiPSC-derived platelets. Platelet pellets were fixed with a mixture of 0.5% glutaraldehyde and 2% paraformaldehyde in 0.1 M phosphate buffer, pH 7.4, for 60 min at 4°C. After washing with phosphate buffer, the samples were post-fixed with 1% osmium tetroxide in phosphate buffer for 60 min on ice. After dehydration, samples on coverslips were infiltrated with and embedded in Epoxy resin. Ultrathin sections (60–80 nm thick) were cut and stained with 2% uranyl acetate in 70% methanol and Reynolds' lead citrate and observed in a transmission electron microscope (1200EX; JEOL) operating at 80 kV.

Flow cytometric analysis of platelets. Washed platelets were prepared as described previously (Takayama et al., 2008). The resultant platelet pellets were resuspended with PBS and stained with anti–human CD41a (integrin αIIb/β3 complex)-APC, GPIX-FITC, GPIbα, or CD9-PE for 30 min at room temperature. The platelets were then diluted in 200 μl PBS and analyzed by flow cytometry. Platelet numbers were estimated using true count beads (BD).

In vitro functional analysis of platelets derived from human iPSCs. Collected platelets were resuspended in an appropriate volume of modified Tyrode-Hepes buffer (10 mM Hepes, pH 7.4, 12 mM $NaHCO_3$, 138 mM NaCl, 5.5 mM glucose, 2.9 mM KCl, and 1 mM $MgCl_2$) and eventually used after addition of 1 mM $CaCl_2$. To investigate integrin αIIbβ3 activation, 50-μl aliquots of fresh PB- or PB-based aged, hESC-, and hiPSC-derived platelets (ESC platelets and iPSC platelets) were incubated with PE-conjugated anti-GPIbα and FITC-conjugated PAC-1 (Shattil et al., 1985) or FITC-conjugated CD62P (P-selectin) in the absence or presence of human thrombin or ADP for 20 min at room temperature. The binding of PAC-1 to platelets was quantified using an Aria flow cytometer. Nonspecific binding was determined in the presence of 10 μM tirofiban, a specific antagonist of human integrin αIIbβ3 (Peerlinck et al., 1993). Specific binding was defined as total minus nonspecific binding.

In vivo imaging by iPSC-platelets. Details of this method are provided elsewhere (Nishimura et al., 2008; Takizawa et al., 2010). In brief, to visually analyze iPSC platelet function, including circulation and thrombus formation in the mesentery of living animals, mice were anesthetized and a small incision was made in the abdominal wall. Intravital imaging was then performed through this small (~3 mm) window. FITC-dextran (20 mg/kg body weight) was injected into the tail vein for visualization of host blood cell dynamics. iPSC-derived platelets were stained with 5 μM TMRE for 15 min, washed, and injected into the mice. To induce thrombus formation, hematoporphyrin (1.8 mg/kg body weight) was also administrated. Sequential two-color images were obtained for 20 s at 30 frames/s using a high-speed spinning-disk confocal laser scanning microscope (CSU-X1) and a pair of EM charge-coupled device cameras (iXon). All experiments were approved by the University of Tokyo Ethics Committee for Animal Experiments and strictly adhered to the guidelines for animal experiments of the University of Tokyo.

Statistical analysis. All data are presented as the mean ± SEM. We used two-tailed Student's *t* tests for statistical analysis; values of $P < 0.05$ were considered significant.

Online supplemental material. Fig. S1 depicts the character of hiPSCs derived from HDFs. Fig. S2 shows the generation of hematopoietic progenitors

from hiPSCs. Figs. S3 and S4 show the time courses of MK generation. Fig. S5 shows the time course of platelet generation. Fig. S6 depicts the representative dot plots of PB-derived and hiPSC-derived platelets. Fig. S7 describes the time-dependent change of exogenous and endogenous c-MYC expression in hESCs and hiPSCs. Fig. S8 shows the in vitro functionality of iPSC platelets. Video 1 shows a typical proplatelet formation. Video 2 demonstrates in vivo imaging of circulating iPSC platelets. Videos 3–5 demonstrate in vivo imaging of iPSC platelet or platelets in thrombi by laser-induced vessel wall injury. Table S1 is a list of primers used in this study. Online supplemental material is available at http://www.jem.org/cgi/content/full/jem.20100844/DC1.

The authors thank Drs. N. Nakatsuji and H. Suemori at Kyoto University for providing human KhES-3 cell lines. 293GPG retroviral packaging cell line was a kind gift from Dr. R.C. Mulligan. Drs. H. Kamiya and S. Yamazaki provided valuable discussion.

This work was supported by Grants-in-Aid from the Ministry of Education, Culture, Sports, Science, and Technology of Japan (The project for realization of regenerative medicine to H. Nakauchi and K. Eto and Kiban B to K. Eto).

N. Takayama, S. Nakamura, H. Nakauchi, and K. Eto have applied for a patent related to the methodology described in the present work. The other authors declare no competing financial interests.

Author contributions: N. Takayama, S. Nishimura, and K. Eto designed the experiments and wrote the manuscript; N. Takayama, S. Nakamura, S. Nishimura, R. Ohnishi, H. Endo, A. Sawaguchi, T. Shimizu, K. Takahashi, and K .Eto performed experiments and analyzed data; T. Yamaguchi, M. Ots, R. Nagai, and S. Yamanaka provided critical reagents and information for the retrovirus system. K. Nishimura and M. Nakanishi made Sendai virus vector for establishment of human iPSCs. S. Yamanaka and H. Nakauchi supervised this research. K. Eto edited the manuscript.

Submitted: 28 April 2010
Accepted: 2 November 2010

REFERENCES

Askew, D.S., R.A. Ashmun, B.C. Simmons, and J.L. Cleveland. 1991. Constitutive c-myc expression in an IL-3-dependent myeloid cell line suppresses cell cycle arrest and accelerates apoptosis. *Oncogene.* 6:1915–1922.

Bergmeier, W., P.C. Burger, C.L. Piffath, K.M. Hoffmeister, J.H. Hartwig, B. Nieswandt, and D.D. Wagner. 2003. Metalloproteinase inhibitors improve the recovery and hemostatic function of in vitro-aged or -injured mouse platelets. *Blood.* 102:4229–4235. doi:10.1182/blood-2003-04-1305

Chanprasert, S., A.E. Geddis, C. Barroga, N.E. Fox, and K. Kaushansky. 2006. Thrombopoietin (TPO) induces c-myc expression through a PI3K- and MAPK-dependent pathway that is not mediated by Akt, PKCzeta or mTOR in TPO-dependent cell lines and primary megakaryocytes. *Cell. Signal.* 18:1212–1218. doi:10.1016/j.cellsig.2005.09.010

Choi, K.D., J. Yu, K. Smuga-Otto, G. Salvagiotto, W. Rehrauer, M. Vodyanik, J. Thomson, and I. Slukvin. 2009. Hematopoietic and endothelial differentiation of human induced pluripotent stem cells. *Stem Cells.* 27:559–567.

Eilers, M., S. Schirm, and J.M. Bishop. 1991. The MYC protein activates transcription of the alpha-prothymosin gene. *EMBO J.* 10:133–141.

Eischen, C.M., J.D. Weber, M.F. Roussel, C.J. Sherr, and J.L. Cleveland. 1999. Disruption of the ARF-Mdm2-p53 tumor suppressor pathway in Myc-induced lymphomagenesis. *Genes Dev.* 13:2658–2669. doi:10.1101/gad.13.20.2658

Eto, K., H. Nishikii, T. Ogaeri, S. Suetsugu, A. Kamiya, T. Kobayashi, D. Yamazaki, A. Oda, T. Takenawa, and H. Nakauchi. 2007. The WAVE2/Abi1 complex differentially regulates megakaryocyte development and spreading: implications for platelet biogenesis and spreading machinery. *Blood.* 110:3637–3647. doi:10.1182/blood-2007-04-085860

Evan, G.I., A.H. Wyllie, C.S. Gilbert, T.D. Littlewood, H. Land, M. Brooks, C.M. Waters, L.Z. Penn, and D.C. Hancock. 1992. Induction of apoptosis in fibroblasts by c-myc protein. *Cell.* 69:119–128. doi:10.1016/0092-8674(92)90123-T

Gawaz, M., H. Langer, and A.E. May. 2005. Platelets in inflammation and atherogenesis. *J. Clin. Invest.* 115:3378–3384. doi:10.1172/JCI27196

Guo, Y., C. Niu, P. Breslin, M. Tang, S. Zhang, W. Wei, A.R. Kini, G.P. Paner, S. Alkan, S.W. Morris, et al. 2009. c-Myc-mediated control of cell fate in megakaryocyte-erythrocyte progenitors. *Blood.* 114:2097–2106. doi:10.1182/blood-2009-01-197947

Kobayashi, T., T. Yamaguchi, S. Hamanaka, M. Kato-Itoh, Y. Yamazaki, M. Ibata, H. Sato, Y.S. Lee, J. Usui, A.S. Knisely, et al. 2010. Generation of rat pancreas in mouse by interspecific blastocyst injection of pluripotent stem cells. *Cell.* 142:787–799. doi:10.1016/j.cell.2010.07.039

Ma, F., Y. Ebihara, K. Umeda, H. Sakai, S. Hanada, H. Zhang, Y. Zaike, E. Tsuchida, T. Nakahata, H. Nakauchi, and K. Tsuji. 2008. Generation of functional erythrocytes from human embryonic stem cell-derived definitive hematopoiesis. *Proc. Natl. Acad. Sci. USA.* 105:13087–13092. doi:10.1073/pnas.0802220105

Miura, K., Y. Okada, T. Aoi, A. Okada, K. Takahashi, K. Okita, M. Nakagawa, M. Koyanagi, K. Tanabe, M. Ohnuki, et al. 2009. Variation in the safety of induced pluripotent stem cell lines. *Nat. Biotechnol.* 27:743–745. doi:10.1038/nbt.1554

Murphy, D.J., M.R. Junttila, L. Pouyet, A. Karnezis, K. Shchors, D.A. Bui, L. Brown-Swigart, L. Johnson, and G.I. Evan. 2008. Distinct thresholds govern Myc's biological output in vivo. *Cancer Cell.* 14:447–457. doi:10.1016/j.ccr.2008.10.018

Nakagawa, M., N. Takizawa, M. Narita, T. Ichisaka, and S. Yamanaka. 2010. Promotion of direct reprogramming by transformation-deficient Myc. *Proc. Natl. Acad. Sci. USA.* 107:14152–14157. doi:10.1073/pnas.1009374107

Nesbitt, W.S., E. Westein, F.J. Tovar-Lopez, E. Tolouei, A. Mitchell, J. Fu, J. Carberry, A. Fouras, and S.P. Jackson. 2009. A shear gradient-dependent platelet aggregation mechanism drives thrombus formation. *Nat. Med.* 15:665–673. doi:10.1038/nm.1955

Nishikii, H., K. Eto, N. Tamura, K. Hattori, B. Heissig, T. Kanaji, A. Sawaguchi, S. Goto, J. Ware, and H. Nakauchi. 2008. Metalloproteinase regulation improves in vitro generation of efficacious platelets from mouse embryonic stem cells. *J. Exp. Med.* 205:1917–1927. doi:10.1084/jem.20071482

Nishimura, K., H. Segawa, T. Goto, M. Morishita, A. Masago, H. Takahashi, Y. Ohmiya, T. Sakaguchi, M. Asada, T. Imamura, et al. 2007. Persistent and stable gene expression by a cytoplasmic RNA replicon based on a noncytopathic variant Sendai virus. *J. Biol. Chem.* 282:27383–27391. doi:10.1074/jbc.M702028200

Nishimura, S., I. Manabe, M. Nagasaki, K. Seo, H. Yamashita, Y. Hosoya, M. Ohsugi, K. Tobe, T. Kadowaki, R. Nagai, and S. Sugiura. 2008. In vivo imaging in mice reveals local cell dynamics and inflammation in obese adipose tissue. *J. Clin. Invest.* 118:710–721.

Okita, K., T. Ichisaka, and S. Yamanaka. 2007. Generation of germline-competent induced pluripotent stem cells. *Nature.* 448:313–317. doi:10.1038/nature05934

Ory, D.S., B.A. Neugeboren, and R.C. Mulligan. 1996. A stable human-derived packaging cell line for production of high titer retrovirus/vesicular stomatitis virus G pseudotypes. *Proc. Natl. Acad. Sci. USA.* 93:11400–11406. doi:10.1073/pnas.93.21.11400

Osafune, K., L. Caron, M. Borowiak, R.J. Martinez, C.S. Fitz-Gerald, Y. Sato, C.A. Cowan, K.R. Chien, and D.A. Melton. 2008. Marked differences in differentiation propensity among human embryonic stem cell lines. *Nat. Biotechnol.* 26:313–315. doi:10.1038/nbt1383

Patel, S.R., J.H. Hartwig, and J.E. Italiano Jr. 2005. The biogenesis of platelets from megakaryocyte proplatelets. *J. Clin. Invest.* 115:3348–3354. doi:10.1172/JCI26891

Peerlinck, K., I. De Lepeleire, M. Goldberg, D. Farrell, J. Barrett, E. Hand, D. Panebianco, H. Deckmyn, J. Vermylen, and J. Arnout. 1993. MK-383 (L-700,462), a selective nonpeptide platelet glycoprotein IIb/IIIa antagonist, is active in man. *Circulation.* 88:1512–1517.

Raya, A., I. Rodríguez-Pizà, G. Guenechea, R. Vassena, S. Navarro, M.J. Barrero, A. Consiglio, M. Castellà, P. Río, E. Sleep, et al. 2009. Disease-corrected haematopoietic progenitors from Fanconi anaemia induced pluripotent stem cells. *Nature.* 460:53–59. doi:10.1038/nature08129

Rylski, M., J.J. Welch, Y.Y. Chen, D.L. Letting, J.A. Diehl, L.A. Chodosh, G.A. Blobel, and M.J. Weiss. 2003. GATA-1-mediated proliferation arrest during erythroid maturation. *Mol. Cell. Biol.* 23:5031–5042. doi:10.1128/MCB.23.14.5031-5042.2003

Schiffer, C.A. 2001. Diagnosis and management of refractoriness to platelet transfusion. *Blood Rev.* 15:175–180. doi:10.1054/blre.2001.0164

Schulze, H., and R.A. Shivdasani. 2005. Mechanisms of thrombopoiesis. *J. Thromb. Haemost.* 3:1717–1724. doi:10.1111/j.1538-7836.2005.01426.x

Shattil, S.J., J.A. Hoxie, M. Cunningham, and L.F. Brass. 1985. Changes in the platelet membrane glycoprotein IIb.IIIa complex during platelet activation. *J. Biol. Chem.* 260:11107–11114.

Takahashi, K., K. Tanabe, M. Ohnuki, M. Narita, T. Ichisaka, K. Tomoda, and S. Yamanaka. 2007. Induction of pluripotent stem cells from adult human fibroblasts by defined factors. *Cell.* 131:861–872. doi:10.1016/j.cell.2007.11.019

Takayama, N., H. Nishikii, J. Usui, H. Tsukui, A. Sawaguchi, T. Hiroyama, K. Eto, and H. Nakauchi. 2008. Generation of functional platelets from human embryonic stem cells in vitro via ES-sacs, VEGF-promoted structures that concentrate hematopoietic progenitors. *Blood.* 111:5298–5306. doi:10.1182/blood-2007-10-117622

Takeuchi, K., M. Satoh, H. Kuno, T. Yoshida, H. Kondo, and M. Takeuchi. 1998. Platelet-like particle formation in the human megakaryoblastic leukaemia cell lines, MEG-01 and MEG-01s. *Br. J. Haematol.* 100:436–444. doi:10.1046/j.1365-2141.1998.00576.x

Takizawa, H., S. Nishimura, N. Takayama, A. Oda, H. Nishikii, Y. Morita, S. Kakinuma, S. Yamazaki, S. Okamura, N. Tamura, et al. 2010. Lnk regulates integrin alphaIIbbeta3 outside-in signaling in mouse platelets, leading to stabilization of thrombus development in vivo. *J. Clin. Invest.* 120:179–190. doi:10.1172/JCI39503

Thompson, A., Y. Zhang, D. Kamen, C.W. Jackson, R.D. Cardiff, and K. Ravid. 1996a. Deregulated expression of c-myc in megakaryocytes of transgenic mice increases megakaryopoiesis and decreases polyploidization. *J. Biol. Chem.* 271:22976–22982. doi:10.1074/jbc.271.38.22976

Thompson, A., Z. Zhao, D. Ladd, J. Zimmet, and K. Ravid. 1996b. A new transgenic mouse model for the study of cell cycle control in megakaryocytes. *Stem Cells.* 14:181–187. doi:10.1002/stem.5530140723

Tomer, A. 2004. Human marrow megakaryocyte differentiation: multiparameter correlative analysis identifies von Willebrand factor as a sensitive and distinctive marker for early (2N and 4N) megakaryocytes. *Blood.* 104:2722–2727. doi:10.1182/blood-2004-02-0769

van der Meer, P.F., and R.N. Pietersz. 2005. Gamma irradiation does not affect 7-day storage of platelet concentrates. *Vox Sang.* 89:97–99. doi:10.1111/j.1423-0410.2005.00647.x

Vodyanik, M.A., J.A. Bork, J.A. Thomson, and I.I. Slukvin. 2005. Human embryonic stem cell-derived CD34+ cells: efficient production in the coculture with OP9 stromal cells and analysis of lymphohematopoietic potential. *Blood.* 105:617–626. doi:10.1182/blood-2004-04-1649

Vyas, P., K. Ault, C.W. Jackson, S.H. Orkin, and R.A. Shivdasani. 1999. Consequences of GATA-1 deficiency in megakaryocytes and platelets. *Blood.* 93:2867–2875.

Wang, L., L. Li, F. Shojaei, K. Levac, C. Cerdan, P. Menendez, T. Martin, A. Rouleau, and M. Bhatia. 2004. Endothelial and hematopoietic cell fate of human embryonic stem cells originates from primitive endothelium with hemangioblastic properties. *Immunity.* 21:31–41. doi:10.1016/j.immuni.2004.06.006

Webb, I.J., and K.C. Anderson. 1999. Risks, costs, and alternatives to platelet transfusions. *Leuk. Lymphoma.* 34:71–84.

Woll, P.S., B. Grzywacz, X. Tian, R.K. Marcus, D.A. Knorr, M.R. Verneris, and D.S. Kaufman. 2009. Human embryonic stem cells differentiate into a homogeneous population of natural killer cells with potent in vivo antitumor activity. *Blood.* 113:6094–6101. doi:10.1182/blood-2008-06-165225

Yokoyama, Y., T. Suzuki, M. Sakata-Yanagimoto, K. Kumano, K. Higashi, T. Takato, M. Kurokawa, S. Ogawa, and S. Chiba. 2009. Derivation of functional mature neutrophils from human embryonic stem cells. *Blood.* 113:6584–6592. doi:10.1182/blood-2008-06-160838

Yu, J., M.A. Vodyanik, K. Smuga-Otto, J. Antosiewicz-Bourget, J.L. Frane, S. Tian, J. Nie, G.A. Jonsdottir, V. Ruotti, R. Stewart, et al. 2007. Induced pluripotent stem cell lines derived from human somatic cells. *Science.* 318:1917–1920. doi:10.1126/science.1151526

Atherosclerosis 212 (2010) 42–47

Contents lists available at ScienceDirect

Atherosclerosis

journal homepage: www.elsevier.com/locate/atherosclerosis

Rapid communication

Sirt1 plays an important role in mediating greater functionality of human ES/iPS-derived vascular endothelial cells

Koichiro Homma[a,e], Masakatsu Sone[a,*], Daisuke Taura[a], Kenichi Yamahara[a], Yutaka Suzuki[b], Kazutoshi Takahashi[c,d], Takuhiro Sonoyama[a], Megumi Inuzuka[a], Yasutomo Fukunaga[a], Naohisa Tamura[a], Hiroshi Itoh[e], Shinya Yamanaka[c,d], Kazuwa Nakao[a]

[a] Department of Medicine and Clinical Science, Kyoto University Graduate School of Medicine, 54 Shogoin Kawahara-cho, Sakyo-ku, Kyoto 606-8507, Japan
[b] Stem Cell and Drug Discovery Institute, Kyoto, Japan
[c] Department of Stem Cell Biology, Institute for Frontier Medical Sciences, Kyoto University, Kyoto, Japan
[d] Center for iPS Cell Research and Application (CiRA), Institute for Integrated Cell-Material Sciences, Kyoto, Japan
[e] Department of Internal Medicine, Keio University School of Medicine, Tokyo, Japan

ARTICLE INFO

Article history:
Received 14 December 2009
Received in revised form 18 March 2010
Accepted 14 April 2010
Available online 22 April 2010

Keywords:
Stem cells
Endothelium
Sirt1

ABSTRACT

Objective: We previously succeeded in inducing and isolating vascular endothelial cells (ECs) from both human embryonic stem (ES) and induced pluripotent stem (iPS) cells. Here, we compared the functionality of human adult aortic ECs (HAECs), human ES-derived ECs (ESECs) and human iPS-derived ECs (iPSECs).

Methods and results: We compared the cell proliferative potential, potential for migration, and tolerance to oxidative stress. ESECs were significantly superior to HAECs in all of these cell functions. The cell functions of iPSECs were comparable to those of ESECSs and also superior to HAECs. We then analyzed the gene expressions of HAECs, ESECs and iPSECs, and observed that the expression level of Sirt1, a nicotinamide adenine dinucleotide (NAD+)-dependent histone deacetylase, is higher in ESECs and iPSECs than in HAECs. The inhibition of Sirt1 with a Sirt1-specific inhibitor and siRNA antagonized these differences between the three types of cells.

Conclusions: Sirt1 plays a key role in the high cellular function of ESECs and iPSECs. Although further in vivo investigations are required, this study initially demonstrated the potential of ESECs and iPSECs as the cell source for regenerative medicine, and also showed the potential of ES cells as a useful tool for elucidating the molecular mechanism of cell aging.

1. Introduction

We have succeeded in selectively inducing mouse, monkey and human ES cells to differentiate into ECs and mural cells and in isolating those cells [1–3]. In addition, we recently succeeded in inducing human iPS cells to differentiate into ECs and mural cells and in isolating those cells [4]. We have also intra-arterially transplanted human ES cell-derived ECs (ESECs) into murine hindlimb ischemia models and found that the transplanted ECs are incorporated into the host vasculature, where they promote the restoration of blood flow. By contrast, almost no transplanted adult aorta-derived ECs were incorporated into the host vasculature, and they did not promote blood flow restoration [3,5]. Other groups comparing the efficiency of engraftment of ESECs and human adult ECs obtained similar results [6–8]. Apparently, there are functional differences between ESECs, which are at a relatively early stage of development, and human adult ECs, which have already been subject to aging.

The aims of the present study were to analyze the functional differences between human adult ECs, ESECs and human iPS cell-derived ECs (iPSECs), to identify factors responsible for these functional differences, and to determine at least part of the mechanism of vascular aging.

2. Methods

2.1. Cell culture

Human adult aortic endothelial cells (HAECs) were purchased from Lonza and maintained in endothelial growth medium (EGM-2, EGM-2 singleQuots, Lonza). Human adult saphenous vein endothelial cells (HVECs) were purchased from VEC Technologies, Inc., and maintained in EGM-2 (EGM-2 singleQuots). The khES1 human ES cell line and the 201B7 human iPS cell line were used and

* Corresponding author. . Tel.: +81 75 751 3170; fax: +81 75 771 9452.
E-mail address: sonemasa@kuhp.kyoto-u.ac.jp (M. Sone).

0021-9150/$ – see front matter © 2010 Elsevier Ireland Ltd. All rights reserved.
doi:10.1016/j.atherosclerosis.2010.04.021

maintained as described previously [4]. Briefly, every 5–6 days, undifferentiated cells of both cell lines were detached with dissecting pipettes and transferred to dishes with mitomycin C-treated mouse feeder cells. All endothelial cells used in this study were not passaged more than five times.

2.2. Induction of differentiation

Undifferentiated human ES or iPS cells were harvested and transferred to a collagen I-coated dish after adjusting the colonies to an appropriate size. On the second day of incubation, the culture medium was replaced with human ES/iPS cell maintenance medium without basic FGF, supplemented with N2 supplement (Invitrogen)/B27 supplement (Invitrogen) and BIO (SIGMA). Thereafter, the cells were incubated for another 3 days, at which time the culture medium was replaced with StemPro-34 SFM (Invitrogen) supplemented with VEGF (50 ng/ml; PeproTech EC Ltd). After another 3–5 days of incubation, Flk1/VE-cadherin+/+ cells were sorted using FACSAria flow cytometer and used for the following experiments. Sorted cells were confirmed to remain VE-cadherin positive during the following cell culture and analyses.

2.3. Immunohistochemistry

Cultured cells were stained with an anti-VE-cadherin antibody (BV-9, Abcam) [9], or the indicated monoclonal antibodies as described [4].

2.4. MTT assay

Cell proliferation was assessed in colorimetric 3,4,5-dimethylthiazol-2-yl-2,5-diphenyl tetrazolium bromide (MTT) assays carried out as described previously [10]. Briefly, cells were incubated with MTT (Nakarai Tesque, Kyoto, Japan) solution for 4 h, after which the medium was discarded. The remaining dye was then dissolved in dimethyl sulfoxide, and the absorbance was measured at 570 nm.

2.5. In vitro wound healing assay

Wound healing assays were carried out as we described previously [11]. Briely, ECs were grown to overconfluence in six-well plates, after which a wound approximately 2 mm in width was made with a cell scraper. The wound was then allowed to heal (re-endothelialize) for 24 h in the same medium. The wounded monolayer was photographed before and after the incubation period, and the area of re-endothelialization was evaluated.

2.6. Annexin V assay

Confluent monolayers (80–90%) of ECs grown in 6-well plates were treated with or without 300 μmol/l H_2O_2. After 8 h of exposure, annexin V-FITC in combination with Via-Probe was used to quantitatively determine the percentage of cells undergoing apoptosis, as described previously [12]. Briefly, after treating the cells with the indicated reagents, the monolayer was detached by a brief incubation with trypsin–EDTA solution. Aliquots of cells (10^5) were then resuspended in 1× binding buffer (BD Pharmingen, San Diego, CA) and incubated with annexin V-FITC for 15 min at room temperature in the dark, stained with Via-Probe, and analyzed within 1 h in a FACSAria flow cytometer. FACS Diva software (Becton Dickinson) was used to analyze the data. Early apoptotic cells were stained with annexin V only, while late apoptotic or necrotic cells were stained with both annexin V and Via-Probe.

2.7. Quantitative real-time PCR

Total RNA was isolated using an RNeasy® Mini Kit and treated with an RNase-free DNase set (QIAGEN, Germany) to remove any contaminating genomic DNA. Quantitative real-time PCR was then performed using Premix ExTaqTM(Takara Bio Inc., Shiga, Japan). The PCR primers used were as follows: for Sirt1, GCCTCACATGCAAGCTCTAGTGAC(forward) and TTCGAGGATCTGTGCCAATCATAA(reverse); for Delta-like 4 (DLL4), GTGGACTGTGGCCTGGACAA(forward) and AGCATATCGCTGATATCCGACACACTC(reverse); for CXCR4, GCCAACGTCAGTCAGTGAGGCAGA(forward) and GCCAACCATGATGTGCTGAAAC(reverse) and for β-actin, CATCCGTAAAGACCTCTATGCCAC(forward) and ATGGAGCCACCATCCACA (reverse). All primers were produced by Takara Bio. Levels of Sirt1, DLL4 and CXCR4 mRNA are presented after normalization to the level of β-actin mRNA.

2.8. Western blot analysis

Western blotting was carried out using a standard protocol described previously [13]. Anti-Sirt1 antibody was purchased from Santa Cruz Biotechnology, Inc.

2.9. siRNA transfection

Small interference RNA (siRNA) against Sirt1 and negative control were provided by Qiagen. The target sequence for the Sirt1 siRNA was 5′CAA GCG ATG TTT GAT ATT GAA3′. ECs were trypsinized, washed with Hank's balanced salt solution, resuspended (5×10^5 cells) in human umbilical vein endothelial cell solution (Amaxa Biosystems) containing 3 μg of siRNA duplex, and then transfected using a Nucleofector (Amaxa Biosystems) following the manufacturer's instructions. After transfection, the cells were immediately plated in dishes.

2.10. Endothelial tube formation assay

Endothelial tube formation was assayed as described previously [14]. ECs (20,000 cells/well) were seeded into matrigel-coated 24-well plates. The cells were then incubated for 12 h at 37 °C, after which the formed tubes were digitally imaged and analyzed using MetaMorph software (Universal Imaging Corp.).

2.11. Statistical analysis

Results are presented as means ± SEM. Differences between groups were analyzed using ANOVA followed by Fisher's analysis for comparisons between two means. Values of $P < 0.05$ were considered significant.

3. Results

3.1. Morphological comparison of HAECs, ESECs and iPSECs

HAECs, ESECs and iPSECs were morphologically similar in that they all exhibited a cobblestone-like appearance on culture dishes, were positive for eNOS, and showed a marginal staining pattern when stained for CD31 and VE-cadherin (Fig. 1). All of these features are characteristic of vascular endothelial cells. Furthermore, HVECs, an example of venous endothelial cells, were analyzed together with HAECs, ESECs and iPSECs by real-time PCR for the expression of arterial endothelial marker genes, DLL4 and CXCR4. The expression levels of DLL4 and CXCR4 in both ESECs and iPSECs were comparable with those in HAECs and higher than those in HVECs